# Distinguishing Lifelong Individual Differences from Divergent Aging Trajectories of Adult Brain Volumes

**Edvard O. S. Grødem[1,2*], Didac Vidal Pineiro[1], Øystein Sørensen[1], David Bartrés-Faz[3,4,5], Andreas M. Brandmaier[6,7,8], Gabriele Cattaneo[4,19], Pablo F. Garrido[1], Richard N. Henson[9], Simone Kühn[8,10,11], Ulman Lindenberger[6,8], Bradley J. MacIntosh[2], Lars Nyberg[1,12,13,14], Alvaro Pascual-Leone[17,18], Stephen M. Smith[20], Cristina Solé-Padullés[3,5], Javier Solana-Sánchez[4, 19], Leiv Otto Watne[15,16], for the Alzheimer's Disease Neuroimaging Initiative[**], for the Vietnam Era Twin Study of Aging (VETSA)[***], Kristine B. Walhovd[1,2], Atle Bjørnerud[2], Anders M. Fjell[1,2]**

***For correspondence:**
edvardgr@uio.no (EOSG)

[1]Center for Lifespan Changes in Brain and Cognition (LCBC), Department of Psychology, University of Oslo, Norway; [2]Computational Radiology and Artificial Intelligence (CRAI), Department of Radiology and Nuclear Medicine, Oslo University Hospital, Norway; [3]Department of Medicine, Faculty of Medicine and Health Sciences, Institute of Neurosciences, University of Barcelona, Barcelona, Spain; [4]Institut Guttmann, Institut Universitari de Neurorehabilitació adscrit a la UAB, Badalona, Spain; [5]The August Pi i Sunyer Biomedical Research Institute (IDIBAPS), Hospital Clinic of Barcelona, Barcelona, Spain; [6]Center for Lifespan Psychology, Max Planck Institute for Human Development, Germany; [7]Department of Psychology, MSB Medical School Berlin, Germany; [8]Max Planck UCL Centre for Computational Psychiatry and Ageing Research, Max Planck Institute for Human Development, Germany; [9]MRC Cognition and Brain Sciences Unit, Department of Psychiatry, University of Cambridge, United Kingdom; [10]Center for Environmental Neuroscience, Max Planck Institute for Human Development, Germany; [11]Department of Psychiatry and Psychotherapy, University Medical Center Hamburg-Eppendorf, Germany; [12]Umeå Center for Functional Brain Imaging, Umeå University, Sweden; [13]Department of Medical and Translational Biology, Umeå University, Sweden; [14]Department of Diagnostics and Intervention, Umeå University, Sweden; [15]Oslo Delirium Research Group, Institute of Clinical Medicine, Campus Ahus, University of Oslo, Norway; [16]Department of Geriatric Medicine, Akershus University Hospital, Norway; [17]Hinda and Arthur Marcus Institute for Aging Research, Deanna and Sidney Wolk Center for Memory Health, Hebrew SeniorLife, MA, United States; [18]Department of Neurology, Harvard Medical School, MA, United States; [19]Fundació Institut d'Investigació en Ciències de la Salut Germans Trias i Pujol, Badalona, Spain; [20]Oxford Centre for Functional MRI of the Brain (FMRIB/WIN), Oxford University, UK

[**]Data used in preparation of this article were obtained from the Alzheimer's Disease Neuroimaging Initiative (ADNI) database (adni.loni.usc.edu). As such, the investigators within the ADNI contributed to the design and implementation of ADNI and/or provided data but did not participate in analysis or writing of this report. A complete listing of ADNI investigators can be found in: http://adni.loni.usc.edu/wp-content/uploads/how_to_apply/ADNI_Acknowledgement_List.pdf

[***]More information about the Vietnam Era Twin Study of Aging (VETSA), including a list of VETSA investigators, is available at: https://psychiatry.ucsd.edu/research/programs-centers/vetsa/

**Abstract** Differences in the volumes of brain structures between individuals are often linked to various conditions, including Alzheimer's disease, schizophrenia, and overall brain health. However, it remains unclear to what extent these differences reflect individual levels present at young adulthood or diverging aging trajectories at later ages. In this study, we analyze the aging dynamics of the volume of six brain structures based on MRI scans from a large cross-cohort

longitudinal sample of cognitively healthy adults (n = 8,311 with 18,520 MRIs, ages from 18 to 97 years). From general assumptions about structural brain dynamics and measurement noise, a stochastic dynamical model was fit to the data to estimate both the variability and persistence of structural changes across adulthood. Using this model, we calculated how much of the variance in individual volumetric differences can be attributed to stable levels from young adulthood versus systematic changes at older ages, as well as the theoretical sensitivity of longitudinal studies to detect individual differences in changes. The findings were as follows: 1) Before age 60 years, inter-individual differences in neuroanatomical volumes almost exclusively reflect stable differences between individuals, while the influence from systematic differences in rate-of-change increases thereafter; up to 40 % of the variation being due to differences in change at 80 years. In contrast, ventricular volume reflects differences in change from early adulthood. 2) Current brain age-models are unlikely to be sensitive to detect differences in aging trajectories. 3) Imaging studies have a low reliability to detect inter-individual brain change before age 60. After 60 years , the study reliability increases sharply with longer intervals between scans and more modestly with additional intermediate observations. In conclusion, it is critical to distinguish stable levels from early adulthood from systematic differences in change when studying adult brain aging.

## Introduction

Adult humans show enormous variation in the size of brain structures within the normal, healthy population. For example, a study found that young healthy adults vary in cortical gray matter volume by 52%, white matter volume by 49% and hippocampal volume by 43% compared to the mean(4 SD / mean) (***Walhovd et al., 2011***). These differences are very large compared to the modest amount of change over time in the same structures when measured longitudinally, which even in old age is less than 1% annually for most regions (***Driscoll et al., 2009***; ***Fjell et al., 2009***; ***Sele et al., 2021***). Thus, it is likely that a major part of volumetric differences in adulthood reflects stable, individual differences originating earlier in life (***Walhovd et al., 2023***). However, the continuous morphological changes throughout life also implies a balance between early adulthood levels and systematic differences in change (aging) contributions with effects of change accumulating over time potentially being more important later in life. Here, we aim to study the degree to which single observations capture early adulthood level vs. change effects in adulthood and how the relative contribution of each change throughout the lifespan.

Due to the greater availability and logistical feasibility of acquiring cross-sectional MRIs (i.e., a single measurement per person), there is considerable interest in estimating individualized aging trends based on cross-sectional observations. Although it is unclear whether these measures can capture the ongoing decline of the brain (***Rohrer, 2025***; ***Raz and Lindenberger, 2011***), such inferences are frequently drawn with respect to brain aging (***Franke and Gaser, 2019***), schizophrenia (***Blake et al., 2023***), brain health (***Bashyam et al., 2020***), a variety of genetic and lifestyle-related risk factors for Alzheimer's disease (AD)(***Habes et al., 2016***), and even mortality (***Cole et al., 2018***).

The assumption that cross-sectional data can be used to index individual differences in change is problematic, because research has demonstrated that cross-sectional differences often do not translate into differences in change (***Nyberg et al., 2021***, ***2010***; ***Raz et al., 2005***) with formal analyses further confirming this weak correspondence (e.g., ***Lindenberger et al.*** (***2011***)). This issue has resurfaced with the increasing popularity of Brain Age Gap (BAG) - often interpreted as a marker of accelerated brain aging and ongoing brain change. However, this interpretation has been repeatedly challenged. Studies show that baseline effects are likely to dominate the BAG signal (***Smith et al., 2019***, ***2025***) and other studies find that there is a modest-to-null correlations between cross-sectional BAG and longitudinal brain change (***Dörfel et al., 2025***; ***Korbmacher et al., 2024***). For example, we previously showed that having a higher BAG was not associated with a faster rate of brain aging, but rather reflected stable differences originating from very early in life (***Vidal-Pineiro***

*et al., 2021*).

It is therefore critical to distinguish contributions from the level at young adulthood vs. systematic differences in change to the total inter-individual differences in brain structure volumes. Importantly, different MRI measures capture ongoing brain changes to varying degrees, with some reflecting change clearly better than BAG (*Smith et al., 2020*; *Vidal-Pineiro et al., 2021*). A recent study found that controlling for intracranial volume (ICV) eliminated a major source of stable brain volume variability, and since the relative contribution of degenerative change to cross-sectional estimates gradually increased with older age, brain volume provides a better reflection of ongoing atrophy when controlling for ICV in older age (*Fürtjes et al., 2024*).

The degree to which accumulation of systematic differences in change eventually manifests itself in observable cross-sectional differences depends on at least three factors:

- The magnitude of the initial differences at young adulthood (level effects).
- The magnitude of the systematic inter-individual differences in change rate (change effects).
- The time span over which the differences in change unfolds.

Thus, individual differences in brain structure at any age will depend on a mixture of stable differences and accumulation of systematic differences in change, and the relative contribution of each is likely vary with age. Estimating how variation in these changes depends on age is also important for designing imaging studies. Several studies have shown, through either simulations (*Brandmaier et al., 2018a*, *2024*) or from empirical data (*Vidal-Piñeiro et al., 2025*), that the magnitude of the true change between measurement is essential for detection of change. Because the rate of volume change in brain structures probably varies with age, the expected signal from change will also vary.

Here, we propose to use a time-dependent stochastic dynamic model of brain volume aging to quantify the relative contributions of levels from young adulthood vs. systematic differences in change to the total variation in six major structural brain measures continuously throughout the adult lifespan. Using stochastic dynamical models to describe systems has a long tradition in physics (*Einstein, 1906*; *Gardiner et al., 1985*), finance (*Lee, 1992*; *Föllmer and Schied, 2011*), engineering (*Kalman, 1960*; *Welch et al., 1995*) and neuroscience (*Friston, 2010*). Due to recent development in Bayesian statistical methods (*Hoffman et al., 2014*), fitting such a system directly from data is now possible within a reasonable computational time-frame (*Driver and Voelkle, 2018*; *Sørensen and McCormick, 2025*).

We hypothesize that the major part of structural brain differences can be explained by inter-individual differences, which remain stable for most of adult life, and that a gradually larger proportion of the variance can be ascribed to individual differences in change at higher ages. To our knowledge, this question has not previously been systematically investigated. We further used the dynamical model to calculate the theoretical correlation between the measurements of brain change with the true (i.e., latent) change, and from this analysis make recommendations for how best design longitudinal studies to maximize sensitivity to ongoing brain change.

## Results

### Method overview

We compiled a dataset of 8,311 cognitively healthy adult participants, totaling 18,520 imaging sessions collected from 14 different longitudinal datasets. Participants ranged in age from 18 to 97 years (3925 males/ 4386 females). T1-weighted MRI scans were processed using FreeSurfer's longitudinal pipeline (*Reuter et al., 2012*), and we extracted volumes for the hippocampus, gray matter, white matter, supratentorial regions (excluding ventricles), lateral ventricles, and the brain stem.

Based on some basic assumption on how the brain structures evolve over time we model the brain as a stochastic dynamical system (*Driver and Voelkle, 2018*; *Murphy, 2023*). We first assume there is a true volume of each individual, independent of measurement noise, which changes continuously over time. The true volume is represented as a latent variable in our model, so we refer

to it as the latent volume. The latent volume changes over time according to a change rate. We assume that the change rate of each individual changes continuously over time and we model this as an accumulation of many random events in addition to a systematic bias that varies smoothly with age. We assume that the contribution to change rate of the these random events are Gaussian distributed. The variance of the random events, which may change smoothly over the lifespan, tells us when individuals are changing their change rate with respect to the rest of the population. We define the age of 18 as the beginning of adulthood, where each individual has a volume for each structure which we refer to as the level at age 18. At his age we assume that the volume of the structures of each individual is linearly dependent on ICV and sex in addition to Gaussian noise. We also assume that the change rate at age 18 years is Gaussian distributed. The measured volume is the latent volume in addition to a bias from imaging site and the measurement noise that is assumed to be Gaussian and independent of all variables. These assumptions lead mathematically to the assumption that the variance of the latent volumes will increase over time, similar to ***Smith et al.*** (***2025***). In our model the mean and the spread of the variance over age is parameterized using splines, therefore our model accounts for non-linear effects effecting the population mean and variance.

The model can evaluate the probability of both a single measurement and a series of longitudinal measurements and therefore both cross-sectional and longitudinal data are used to fit the model. The model is generative, meaning it can simulate data, and has its parameters inferred from real data using Bayesian methods (***Hoffman et al., 2014***). The Bayesian framework gives the uncertainty for all parameters of the model, including the interaction between different parameters (***McElreath, 2018***).

As a result, our model provides, across all ages, estimates of the population mean and variance for:

- The brain structure volume
- The change rate of the brain volume (first derivative / velocity)
- The change rate of the change rate of the brain volume (second derivative / acceleration)

## Dynamical Aging Norm Curves for Brain Structures

Fig.1 provides an overview of the aging of the brain structures across the the adult lifespan. The mean and two standard deviations around the mean are plotted for both the latent volume and the change rate. The mean trajectories of the volumes show distinct shapes. The hippocampal and the supratentorial volume gradually decrease until around 55 years of age, followed by an acceleration of change rate and therefore faster shrinkage after age 60 years. The white matter and the brain stem volume follow similar mean trajectories, with an increase in volume up to the age of 50 years, followed by decline. Gray matter volume shows a steady, close to linear, shrinkage throughout life. The lateral ventricles follow a very different trajectory. Most people start with small lateral ventricles at the age of 18 and there is a small but measurable increase up to 50 years. After that, the rate of growth accelerates, leading to a rapid increase in size.

Although the mean trajectories differ across structures, the variation in change rate follows a similar pattern. For all structures, the variation in change rate is very small up to the age of approximately 45 to 50 years. This implies that the inter-individual differences in change for an age can be small even though the change rate might be high, as seen in the case for gray matter. After the age of 50 years, the variation in change rate increases, which after a few decades results in a moderate spread of the observed volumes. The lateral ventricles follow a different pattern. Already from young age there are observable inter-individual differences in change rate, and later in life there is large spread of both the change rate and the volume.

## Explained Variance from Young Adult Levels vs. Systematic Change

We quantified how much variance in brain-structure volume at later ages can be explained by the volume measured at age 18. From the fitted model we calculated the squared correlation,

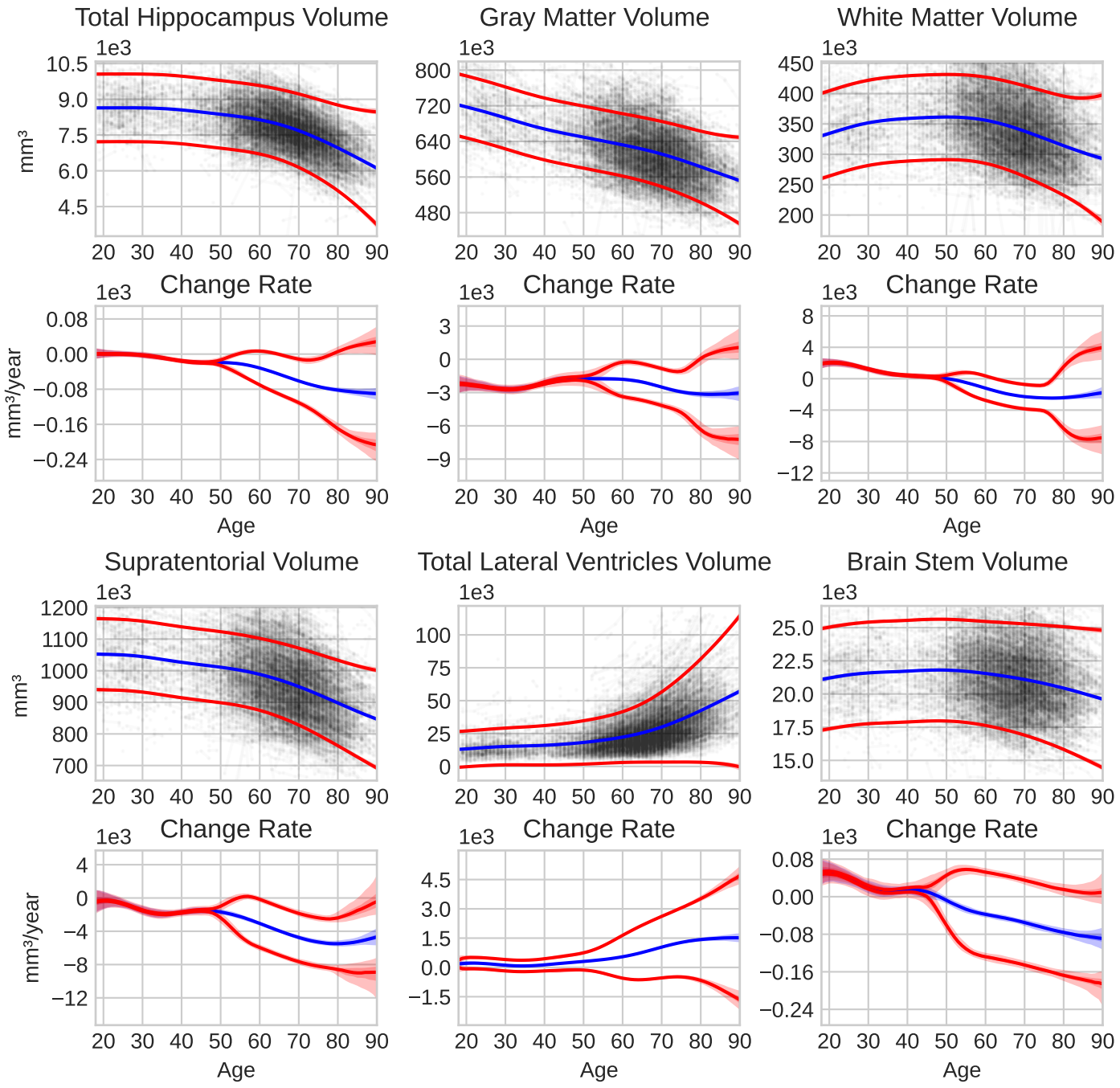


**Figure 1.** Norm curves for the dynamics of selected brain structures. For each structure the top plot shows the latent structure volume for the population from age 18 to 90, and the bottom plot the change rate of the latent volume. The observed data is plotted in the background. The blue curves indicates the population mean and the red curves show two standard deviations from the population mean, meaning ~95% of the population is expected to have volumes and change rates within this region. The shaded region indicate the 50% and the 95% confidence interval (CI) for each curve. For some curves the CI are small, and therefore the CI regions appears as a single line.

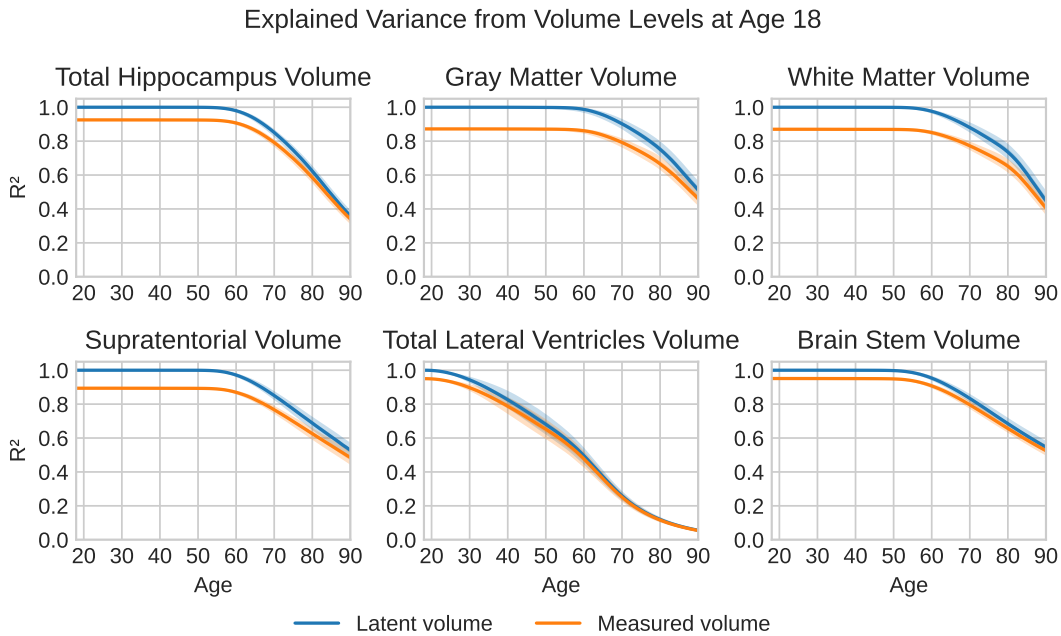


**Figure 2.** The ratio of explained variance $R^2$ in brain structure volumes across the lifespan, given the structure volume at age 18 years. A value of 1 indicates perfect correlation later in life with the volume at age 18 years. The blue line shows the explained variance of the latent volumes without measurement noise, while the orange line includes measurement noise. Both lines are calculated from the fitted model. Confidence intervals are shown as shaded regions around each line; however, in most graphs, the intervals are narrow and appear as lines rather than shaded areas. We refer to the Methods and Materials where the calculations are explained in detail. In this plot $\rho^2_{s_k s_{k+n}}$ and $\rho^2_{\hat{s}_k \hat{s}_{k+n}}$ with $t_k = 18$ years of Eq. 17 are visualized.

corresponding to the proportion of explained variance, $R^2$, between individuals at age 18 with the same individuals later in life. To maximize sensitivity to true change, ICV and sex were regressed out. The calculations were performed both with and without measurement noise. That is; without noise the $R^2$ reflects the explained variance of the *latent* volume in life given the sex, ICV and *latent* volume at 18 years. With noise, the $R^2$ reflects the explained variance of the *measured* volume later in life given the sex, ICV and *measured* at age 18.

The proportion of explained variance is shown in Fig. 2. We observe that up to the age of 60 years, the initial volumes explained nearly all of the variance. For instance for hippocampal volume at age 50 years, the model predicts that the initial latent volume explains 99.9% of the variance, while a measured volume explained 92.4%. At age 60 years, 97.9% of the explained variance in the latent volume is from young adult levels. This number then drops rapidly with the large increase in systematic differences in volumetric change to age 90 years where only 35.8% of the variance is explained by young adult levels.

The other structures show similar trends. The exception is again the lateral ventricles which shows a steady decrease in correlation with the initial volume throughout the age-range, i.e. effects of differences in change are observed at earlier ages. At age 40 years, the explained variance from the ventricle volume at age 18 years is 83.0 % which drops steadily to age 90 years where the initial volume only accounts for 5.6% of the variance.

## Stability of Individual Change Rates Over the Lifespan

The change rate of an individual is often assumed to be stable over time. Changes earlier in life are also often assumed to predict changes later in life. We tested whether an individual's rate of brain-volume change remains stable over time by calculating the auto-correlation (AC) of latent change rates. AC reflects the correlation between a person's change rate at one age and the same

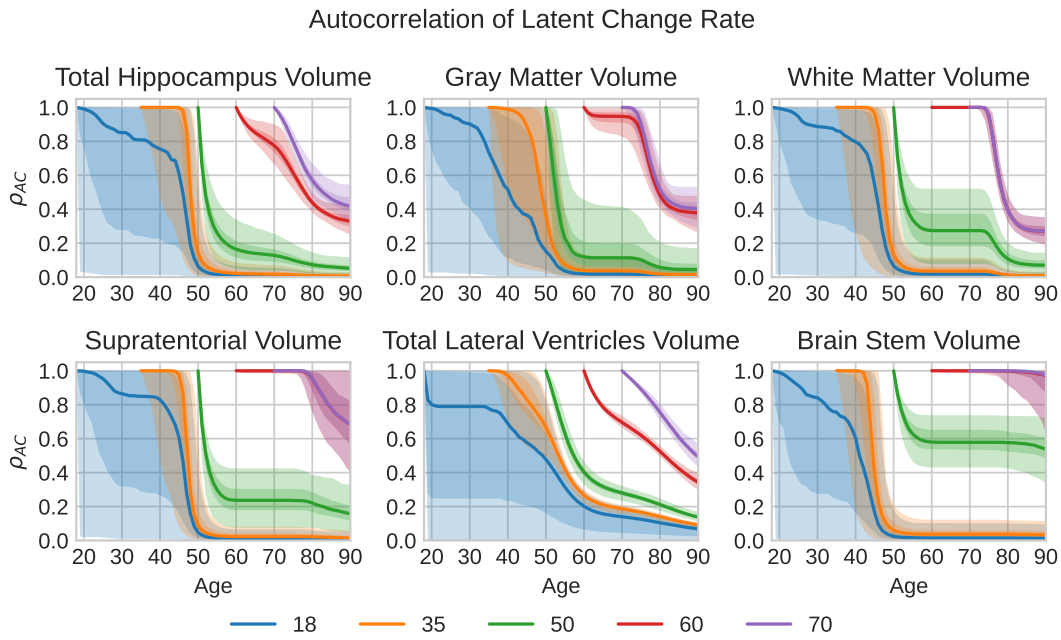


**Figure 3.** Auto-correlation $\rho_{\text{AC}}$ of latent brain volume change rates across the lifespan. AC reflects the correlation between an individual's change rate at a given baseline age and their change rate at later ages. Each colored line represents a different baseline age ($t_k$), as indicated in the legend. By definition, all lines start at AC = 1.0 at their baseline age and then decline as the temporal gap increases. A steeper decline and lower values indicates less stability in individual change rates over time. The shaded regions show the 95% and 50% confidence intervals for each estimate. See Methods and Materials for details on the AC calculation, which corresponds to $\rho_{v_k v_{k+n}}$ in Eq. 17 where each line represents a different $t_k$.

person's change rate at a later age. This indicates the extent to which a perfect measurement of latent change at one age can predict the rate of latent change later in life.

We calculated the AC between the ages of $[18, 35, 50, 60, 70]$ and all subsequent ages (Fig. 3). Under the age of 40 years, the CI of the AC is wide, indicating that we lack sufficient statistical power to estimate the AC for these ages. However, we observe that there is no correlation between the change rate at 35 years and that of later ages, indicating that a change measurement at 35 has little predictive value for later life. At age 50 years, the change rate has a weak correlation with the change rate at later ages. For instance, the AC of hippocampal change rate between age 50 and 70 is around $0.15$. This means that even with a perfect measure of change rate, prediction of change 20 years later is poor. At higher ages and with shorter intervals, the correlations are substantially higher—around $0.80$ from 60 to 70 years, and $0.40$ from 60 to 80 years for the hippocampus. For the supratentorial and brain stem volumes, the change rates at age 60 years show near-perfect correlation with the change rate at 80 years. As we will discuss later, this may likely be a model artifact, due to the lack of feedback in the model. We therefore highlight that these correlations are likely inflated.

## Estimation of Change Rate

As the brain ages, accumulated differences in anatomical changes affect overall brain volume. Consequently, a single volume measurement — when compared to the age-group norm — can serve as an estimate of the current rate of change. However, earlier changes may not accurately reflect the current rate, and the accumulated changes might be too small compared to measurement noise for the volume to be related to the current change rate. To evaluate how well a single volume measurement of brain volume can act as a proxy for the current change rate, we computed the correlation between the measured volume at a given age and the latent change rate.

An alternative method for obtaining an estimate for the change rate is to take the difference between two volume measurements, which we call a delta estimate. From the model we calculated the correlation between the delta estimate and the latent change for different time intervals between the measurements.

The resulting correlations are shown as black lines in Fig. 4. Up to the age of 50 years, there is no correlation between measured volume and change rate, except for the lateral ventricles where the correlation is approx. $0.4$ at age 40 years. At older age, the measured volume is moderately correlated with the change rate. For instance at age 80 years a measurement of the hippocampus volume has a $0.45$ correlation with change rate.

The delta estimates of change rate show a similar trend with no correlation up to age 50. After this age, delta estimate for 1 year and 2 year between-scanning intervals show in general a lower correlation with the latent change rate than a volume measurement. For instance, a 2 year delta estimate of hippocampus at age 70 years has a correlation of about $0.25$ with the latent change rate, while a volume measurement has a correlation of about $0.35$. This means that if the follow-up interval between MRIs at age 70 is 2 years or less, a cross-sectional scan may give slightly better estimates of ongoing atrophy than using estimates from the longitudinal scans. With 8 years or more between scans, however, the delta estimate of change does in general outperform the single volume estimate of change. Interestingly, we see the largest benefit from longitudinal observations compared to a single observation at the age of the beginning of accumulation of inter-individual differences in change, between 50 and 60 years. Here, while still having a low correlation with true change rate, a two-year observation interval captures the change rate more accurately than a single volume measurement. The reason is likely that at this age, we are able to measure individual differences in change with a certain degree of accuracy, while the effects of accumulated change on the observed volumes are still too small compared to the stable individual differences to be detected in a cross-sectional analysis. When differences in change accumulate over time, however, effects on volume increase to a level where they can be measured with higher accuracy than actual longitudinal changes.

Instead of increasing the time interval, one can increase the number of scans within the time interval to obtain a better estimate of the change rate using the slope of a linear model fitted to the measured volumes (***Elliott et al., 2025***). The correlation of the slope estimate with the true change rate can be calculated analytically (***Brandmaier et al., 2018a***; ***Vidal-Piñeiro et al., 2025***). We assume that all the imaging sessions are equally spaced in time, and that the measurement errors are uncorrelated, which is the best case scenario, since in reality the noise is likely correlated between sessions (***Elliott et al., 2024***). We then calculated the theoretical correlation given 2, 6, or 12 imaging sessions within one 1, 2, or 4 years. The resulting correlation curves can be seen in Fig. 5.

We observe that increasing the number of sessions, even under the assumption of perfect uncorrelated measurement noise, only shows a moderate increase in correlation compared to increasing the time between the first and the last session. For instance, for a 2-year measurement interval for hippocampal volume at age 80 years, the correlation with the change rate is 0.38 using 2 measurements and 0.47 using 12 measurements within the same scanning interval. This improvement is lower than for going from 2 to 4 year intervals with only two scans, where the correlation improves from 0.38 to 0.62.

From our calculations, increasing the number of sessions from 2 to 12 is almost never as good as doubling the time between two measurements. The take-home-message is that increasing the signal, i.e. the absolute amount of change, is more efficient than adding more measurements. Note that these calculations assume equal spacing between each measurement, and the situation will be different if multiple measurements are performed close to the first and the last timepoint.

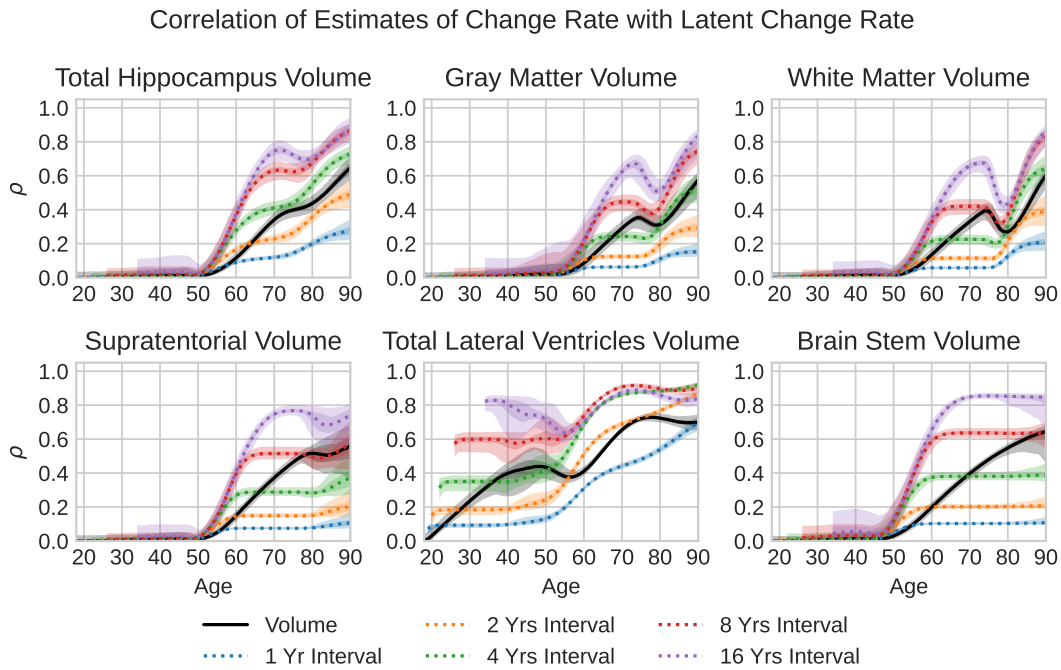


**Figure 4.** The correlation $\rho$ between measured volume with the latent change rate, and the correlation of the delta estimate with latent change rate. The black line indicate the how much a measurement of the volume of a brain structure correlates with the latent change rate of that volume at that time point. The colored lines indicates how much the the slope between two longitudinal measurements of brain volume correlates with the latent change rate of that volume at the last session. Each color indicate the time between the sessions. The shaded regions show the 95% and 50% confidence interval of each line. In the Methods and Materials section the black lines corresponds to $\rho_{v_k s_k}$ of Eq. 17 with $n = 0$ and the colored lines corresponds to $\rho(\hat{v}_{k+n}, v_{k+n})$ of Eq. 20.

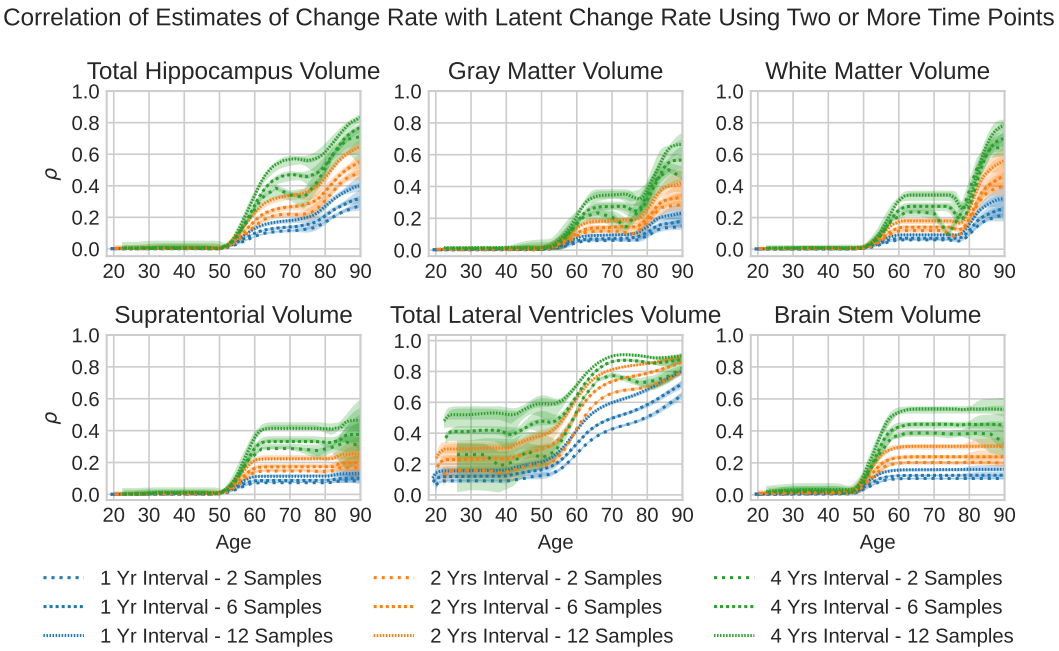


**Figure 5.** The correlation $\rho$ between slope estimates of change rate from 2, 6 and 12 sessions with the latent change rate. The 2 samples lines are the same as the colored lines in Fig. 4 while the other lines indicate the correlation between the slope estimate with the latent change rate when including more intermediate sessions. In the Methods and Materials section these correlations are calculated from Eq. 23.

## Discussion

The present analyses yielded three main results. First, we are not able to detect systematic inter-individual differences in volumetric brain change before age 50 years in a large cross-cohort sample of cognitively healthy adults. This indicates that in cognitively healthy adults, morphometric differences prior to age 50 years largely reflect stable individual differences, and cannot be ascribed to differences in change rate. From about 60 years, individuals started to follow detectable different trajectories, and differences in change gradually explained more variance with higher age. Second, because the variation appears to be dominated by stable individual differences, a model trained to predict cross-sectional age will be sensitive to age, but not differences in aging. The only measure partially reflecting individual differences in change before age 60 was the ventricles, which are known to be sensitive to age-related changes, but typically do not dominate in brain age calculations. Finally, the reliability to detect differences in change was very low before age 50 years, even with many samples and up to 16 years between first and last measurement. From the age of 50 years, reliability increases with longer follow-up times having the largest effects, while adding more intermediate time-points comparatively affected reliability to a very modest degree. For example, two scans 4 years apart yielded similar or higher reliability to detect change than 12 scans evenly distributed over 2 years. The implications of the findings are discussed below.

### Cross-sectional differences mostly do not reflect differences in brain change

The aging norm trajectories of the different brain structures replicate previous aging studies (***Fjell et al., 2013***). All the structures showed age-related decline, but followed distinct patterns. The hippocampus remains relatively stable until around 60 years of age, after that accelerated decline is observed. In contrast, total gray matter volume exhibits almost linear reductions, with a slight acceleration from age 60 onward. White matter and brain stem are the only structures not showing monotonic decline, instead apparently increasing until middle age, which is a well-established pattern (***Walhovd et al., 2005***; ***Allen et al., 2005***). The lateral ventricles display the most unique

trajectory, with a small increase in volume until around 50 years, followed by a rapid increase throughout the rest of the lifespan.

Importantly, as was recently demonstrated in a study of the UK Biobank database, high cross-sectional age correlations do not necessarily translate to high sensitivity to brain change (***Smith et al., 2025***). This means that if individuals have smaller volume of an age-sensitive brain structure, this does not imply that they have undergone greater age-related changes than others. The present results clearly confirm that while brain regions may be age-sensitive at the group level, this does not reflect the existence of systematic differences in age-related rates of change (***Vidal-Piñeiro et al., 2025***). We observe substantial age-related changes in all tested neuroanatomical volumes, with some, particularly total gray matter volume and supratentorial volume, changing continuously from early adulthood. Nevertheless, the variance attributable to baseline differences surpasses the variance associated with individual differences in change by far, at least until advanced ages.

As shown in Figure 2, until around 60 years of age, nearly all differences in neuroanatomical volumes reflect stable, individual differences established in early adulthood. From approximately 50 years, systematic differences in change rates between participants become detectable. These differences accumulate over time, and by 60 years, their impact is sufficiently large to be observed as smaller volumes, but only a minor proportion of individual variation is still due to systematic differences in change. This proportion steadily increases at different rates across structures, reaching approximately 20% at 70 years and up to 50% or more at 90 years for most structures. It is crucial to note that these findings represent group-level effects and cannot be directly translated into considerations on level versus systematic change in the brains of individual participants.

The reason for the small proportion of variance attributed to systematic differences in change is that absolute volumetric differences between individuals are substantial, while inter-individual variation in change is relatively small. Consequently, only after several decades do volumetric differences significantly reflect change. However, the ventricles deviated from this pattern, and we are able to detect small individual changes during the first 30 years of adulthood before expanding rapidly from around 50 years. The relatively minor individual differences in baseline volume, combined with systematic variation in individual change rates, also at young age, result in a situation where a much larger proportion of volume variation can be attributed to change. Even at 50 years, more than a quarter of the volumetric differences between individuals can be explained by differences in change, a proportion that reaches nearly 95% at 90 years. This means that ventricular size is the only tested brain measure that reflects actual age-related variability when measured at a single time point throughout life. This observation was previously reported by ***Vidal-Pineiro et al.*** (***2021***).

Thus, measures where the rate of change later in life is large relative to inter-individual variation in young adulthood will, by this reasoning, reflect proportionally more change than baseline effects when measured in aging. Another good example is white matter hypointensities, not measured here, where variation appears to reflect change to a greater extent than most other brain measures (***Smith et al., 2025***). However, this also means that for other brain measures, cross-sectional comparisons do not inform us about individual differences in aging in cognitively healthy normal populations. Hence, typical brain age models, trained to predict chronological age, will typically be dominated by cross-sectional variance and consequently very insensitive to individual differences in rate of aging (***Smith et al., 2025***).

## Impact of levels vs. change will depend on the sample

An important consideration is that the proportion of variance at a given age that can be attributed to levels at young adulthood vs. systematic differences in change will depend on the type of samples included. For example, we find that about 40% of the individual differences in hippocampal volume at age 80 years can be ascribed to differences in change, but this number is likely much higher in neurodegenerative disorders like AD. While we estimate annual change in hippocampal volume to be around 1% after 60 years, this number often exceeds 3.5% in AD patients (***Fjell et al.,***

***2009***). Consequently, such a large difference in rate of atrophy will eventually manifest in lower hippocampal volume in AD patients, regardless of the variation at young adulthood. Although large baseline hippocampal volume may be a protective factor, volumetric differences between patients with progressed AD and age-matched controls will likely to a larger extent reflect accumulated higher atrophy rates in the patients. How much of the variance that can be ascribed to each remains to be tested. Similarly, comparing other patient groups having conditions associated with magnified volumetric change rates may also be expected to yield a higher proportion of volumetric differences ascribed to change.

Still, AD and some other age-related dementias are extreme cases, as they are characterized by massive neurodegeneration. For many other conditions where neuroanatomical differences are found — such as neuropsychiatric disorders like schizophrenia (***Constantinides et al., 2023***; ***Van Erp et al., 2018***; ***Zhu et al., 2023***) or major depression (***Han et al., 2021***), differences in change rates are usually much smaller (***Abé et al., 2022***; ***Vita et al., 2012***) than in AD. In such cases, the present results suggest that volumetric differences largely reflect stable levels, likely originating early in life and possibly partly due to developmental differences.

For example, a large multi-sample study of bipolar disorder did not find substantial differences in change rates of neuroanatomical volume between patients and controls (***Abé et al., 2022***). Therefore, a cross-sectional comparison would be expected to reveal primarily level differences between groups, regardless of the age at testing. However, this study included several middle-aged and older participants and higher ventricular expansion was observed in the patient group. This finding is particularly relevant, as ventricular expansion was the one variable in the present study that reflected the most systematic differences in change.

Other cross-sectional studies of schizophrenia have found that patients have higher predicted brain age than controls (***Constantinides et al., 2023***). As argued above, brain age prediction models depend on age relationships and, therefore, primarily reflect the features of brain structures that are most reliably linked to age. For example, total gray matter volume would typically be assigned high weight in brain age models, and has been reported to be the measure most predictive of brain age differences between patients with schizophrenia and controls (***Ballester et al., 2023***). However, as low inter-individual differences in change give more precise brain age predictions, such measures are likely insensitive to aging (***Smith et al., 2025***). An implication is that cross-sectional studies of aging differences between neuropsychiatric groups run a high risk of confounding stable levels with true aging effects.

Education, sometimes regarded as one of the strongest protective factors for dementia (***Livingston et al., 2024***), has recently been shown to correlate with larger brain volumes but not differences in brain change (***Nyberg et al., 2021***). Longitudinal and cross-sectional brain structural measures are also found to relate differently to cognitive function (***Walhovd et al., 2022***). These results fit well with the present observation that differences in regional brain volumes mostly reflect stable individual differences also in relatively high age.

Conversely, when comparing groups with different clearly defined developmental risk factors, such as prenatal drug or alcohol exposure, very low birth weight or premature birth, brain volumetric differences will probably for even longer reflect effects present early in life. Consistent with this, a review showed that reported effect sizes on neuronataomical volumes from fetal life risk factors were several times larger than later-life risk factors such as hypertension, overweight and heavy alcohol consumption (***Walhovd et al., 2023***). We expect the same to be the case with neurodevelopmental psychiatric diagnoses associated with brain morphometric differences, such as attention deficit hyperactivity disorder (***Hoogman et al., 2017***). Since these differences also originate from early in life, adult comparisons will be expected to primarily reflect stable levels even in old age (***Walhovd et al., 2012***).

## Implications for studies of brain aging

The results confirm a growing body of evidence suggesting that deviation from "age-expected" lifespan brain trajectories cannot be used to make inferences about brain aging, at least not before the age of 60. Cross-sectional studies can provide important information about the brain basis for cognitive function in aging, but brain aging per se is better studied using longitudinal designs. Interestingly, the results suggest that we have very little signal to detect systematic differences in brain change before the age of 50 years, although this will ultimately depend on the reliability of the measurements (signal-noise ratio) (***Brandmaier et al., 2018b***; ***Vidal-Piñeiro et al., 2025***) and the sample in question.

As has been shown previously using simulations (***Ghisletta et al., 2020***; ***Brandmaier et al., 2024***) and computations based on empirical data (***Hertzog et al., 2008***; ***Vidal-Piñeiro et al., 2025***), the results show that time between measurements is much more important for reliability than the number of observations. Except for the lateral ventricles, reliability was low even with 12 scanning session evenly spaced across 12 months. In contrast, a 4 year follow-up interval increased reliability greatly. This demonstrates that more signal is the most important factor for reliable measures of longitudinal brain change. Since change rates increase with age, the reliability also increased greatly with aging, reaching a correlation of about $0.70$ for hippocampal change over four years even with only two scans. Hence, an implication for aging studies is to maximize follow-up time even at the expense of more time-points.

An exception to this conclusion is of course when special events are of interest, such as in intervention and experimental studies, which differ from observational studies of naturally occurring aging processes. For example, intervention studies have detected systematic effects of cognitive training over a few weeks in younger and older participants (***Engvig et al., 2010***; ***Wenger et al., 2012***, ***2017***; ***Bråthen et al., 2022***). In these cases, post-intervention differences reflect change due to the experimental intervention. Another reason to prefer many imaging sessions is that participants are likely to drop out of the study, and acquiring intermediate sessions might be necessary to ensure some data before participants potentially drop out.

Another implication is that if only cross-sectional data are available, aging studies should focus on brain measures reflecting differences in change to a larger degree, e.g. the lateral ventricles and WM hypointensities (***Smith et al., 2025***; ***Vidal-Pineiro et al., 2021***). Similarly, residualizing total brain volumes for ICV has been shown to correlate with ongoing atrophy (***Fürtjes et al., 2024***), because these measures are very highly correlated in adolescence and young adulthood, and residual scores therefore partially reflect accumulated change since lifetime peak brain size. In any case, the results underscore the need to consider early-life developmental processes to understand and account for individual differences in brain structure at all later stages in life (***Walhovd et al., 2016***).

## Considerations and limitations

Our results rely on the accuracy of the assumptions we use to construct our model. First, we assume that the measurement noise is Gaussian distributed and independent of all variables. This may not be true as older individuals are harder to scan due to factors such as movement (***Vidal-Piñeiro et al., 2025***). Second, we also assume the noise driving the stochastic part of the acceleration to be Gaussian distributed. It is likely that the true distribution of change rate and acceleration is skewed as is shown in ***Vidal-Piñeiro et al.*** (***2025***). Third, similar concerns can be raised for the initial distributions of structure volume and change rate, which we assumed are Gaussian distributed. For the lateral ventricles, it is especially evident that this does not hold, which can be seen in Fig. 1, where the 95% CI of the population also includes negative ventricle volumes.

However, there are also good reasons for assuming a Gaussian distribution. First, this makes the model analytical, such that the probability of multiple observations of a single individual as well as all the results presented in Fig 1 to 5 can be calculated directly from the model parameters. Second, Gaussian distributions can also be considered the base assumption. Keep in in mind that most other models, such as Latent Growth Curve Models (***Preacher, 2008***) and the model used by

***Smith et al.*** (***2025***) are based on Gaussian distributions.

We are also assuming that the dataset population is representative, also for each age group. We have attempted to compensate for cohort effects by regressing out ICV, however, some cohort effects between datasets and age groups may still exist.

The small variance of the population change rate up to the age of 50 years may seem unlikely, as this suggests that all brain structures are changing at the same rate between individuals. Since we assume that acceleration is independent of change rate and volume, this implies that the population variance must increase over time(see the Materials and Method sections for details). A visual inspection of Fig. 1 as well as Appendix 5 Fig 1 shows that the variance at age 50 years is similar to that of age 18, and therefore, according to our assumption, there must be little individual differences in change rate. In reality there might be some interaction between acceleration and change rate, for instance is it observed that an increase in regional brain volume is followed by a decrease later (***Engvig et al., 2010***; ***Wenger et al., 2012***, ***2017***; ***Bråthen et al., 2022***), which would correspond to a negative feedback effect from change rate or volume to acceleration. This would allow individuals to have larger differences in change rates, with smaller increases in the volume population variance than what is possible in our model. In Fig. 3 we see that there is perfect correlation between the change rate of the supratentorial volume at age 60 years and all the way to age 75. This is an also an unlikely scenario, that we believe also rises from the lack of feedback. The model observes little acceleration of the spread of the data, and the most probable fit is therefore that the change rate at 60 is maintained to the age of 75. With feedback the volume change rate of individual would fluctuate towards the population mean, while the correlation the change rate between two ages would go down.

We must therefore emphasis that these results only hold as long as the model assumptions hold. The correlations are likely to be slightly inflated dude to the lack of feedback. However, due to the small amount of widening of the variance with age we believe that the results still largely gives an accurate description of the proportion of variance in brain volumes contributed from adulthood change.

### Conclusion and further research

The present results show that at up to age 50, there are small systematic differences in change for brain structures between individuals. After age 50, larger systematic differences in changes begin to accumulate, resulting in a gradual increase in brain neuroanatomical differences, and in observed volumetric differences at age 60. Therefore, before the age of 60 years, differences in brain volumes primarily reflect stable levels from young adulthood. The proportion of variance attributable to systematic differences in change increases at higher ages, typically reaching 30-40% at age 80 years and 50-65% at age 90 years. The exception is ventricular volume, with more than 70% of the individual differences in volume at age 70 years reflecting differences in change, a proportion increasing to 90% at age 80. Further research should extend these findings to include different populations, including neuropsychiatric conditions, groups with different risk factors, and diseases known to affect brain structure. It will be important to assess how the relative contributions from levels of young adult vs. differences in change varies as a function of various diseases and conditions.

## Methods and Materials

### Data

We compiled a dataset from 14 different datasets, with a combined 8,310 subjects with a total of 18,520 sessions. Both longitudinal and cross-sectional data was in included in the analysis. Table 1 gives lists the datasets used in this study.

The age distribution of the datasets is shown in Fig. 6. See Supplementary information of ***Vidal-Piñeiro et al.*** (***2025***) for an detailed overview of each dataset.

| Dataset | Abbreviation | Reference | N subjects | N sessions |
|---|---|---|---|---|
| UKBiobank | UKB | ***Miller et al.*** (***2016***) | 1287 | 2574 |
| UiO LCBC | LCBC | ***Walhovd et al.*** (***2018***) | 1274 | 2295 |
| OASIS-3 | OASIS-3 | ***LaMontagne et al.*** (***2019***) | 974 | 2120 |
| The Barcelona Brain Health Initiative | BBHI | ***Cattaneo et al.*** (***2018***) | 930 | 1201 |
| The Alzheimer's disease neuroimaging initiative | ADNI | ***Mueller et al.*** (***2005***) | 769 | 3316 |
| Cambridge Centre for Ageing Neuroscience | Cam-CAN | ***Shafto et al.*** (***2014***) | 638 | 905 |
| The Berlin Aging Study II | BASE-II | ***Bertram et al.*** (***2014***) | 430 | 730 |
| The Vietnam Era Twin Study of Aging | VETSA | ***Kremen et al.*** (***2019***) | 406 | 1453 |
| The Wayne State longitudinal data set | Wayne | ***Kennedy and Raz*** (***2009***); ***Burgmans et al.*** (***2010***) | 313 | 497 |
| PREVENT-AD | Prevent-AD | ***Tremblay-Mercier et al.*** (***2021***) | 305 | 1360 |
| The BETULA project | BETULA | ***Nilsson et al.*** (***1997***, 2004) | 303 | 587 |
| The University of Barcelona | UB | ***Rajaram et al.*** (***2017***); ***Vidal-Piñeiro et al.*** (***2014***); ***Abellaneda-Pérez et al.*** (***2019***); ***Uribe et al.*** (***2016***) | 288 | 421 |
| Harvard Aging Brain Study | HABS* | ***Dagley et al.*** (***2017***) | 281 | 673 |
| COGNORM | COGNORM | ***Idland et al.*** (***2017***) | 113 | 388 |

**Table 1.** List of datasets used in the study. *HABS data release 2.20, retrieved in August 2022 via habs.mgh.harvard.edu.

The T1-weighted MRI brain scans of each individual were processed with longitudinal FreeSurfer v.7.1.0 stream (***Reuter et al., 2012***). The volume of combined hippocampus, gray matter, white matter, supratentorial regions (excluding ventricles), combined lateral ventricles, and the brainstem was extracted. We also used the imaging site a covariate in out model. In the ADNI dataset, some sites have very few participants, we therefore constructed combined sites for ADNI after scanner type. This reduces the total number of imaging sites from $125$ to $39$.

## Model

No study follows individuals longitudinally from early adulthood through old age. Therefore, we construct a dynamical model to understand brain development over the lifespan. Our approach is based on several assumptions that enable us to characterize the evolution of brain structure volumes under both systematic trends and random variations. Brain structures, such as the hippocampus, changes gradually over time; abrupt changes in volume are not expected. We also expect the change rate of each structure to be stable over a short time span. However, over a lifetime an individual may change their change rate relative to the population, due to external factors such as lifestyle, illness or other random influences. We assume that the change rate at any given time reflects the cumulative effect of numerous random events throughout life, along with a systematic influence related to aging. Furthermore, we assume that the change rate of the change rate (i.e. the acceleration) itself is not directly driven by the current volume or the current change rate. We argue that this assumption is justified in adult populations where the rapid growth phase has already concluded. We also address differences among cohorts by considering the intracranial

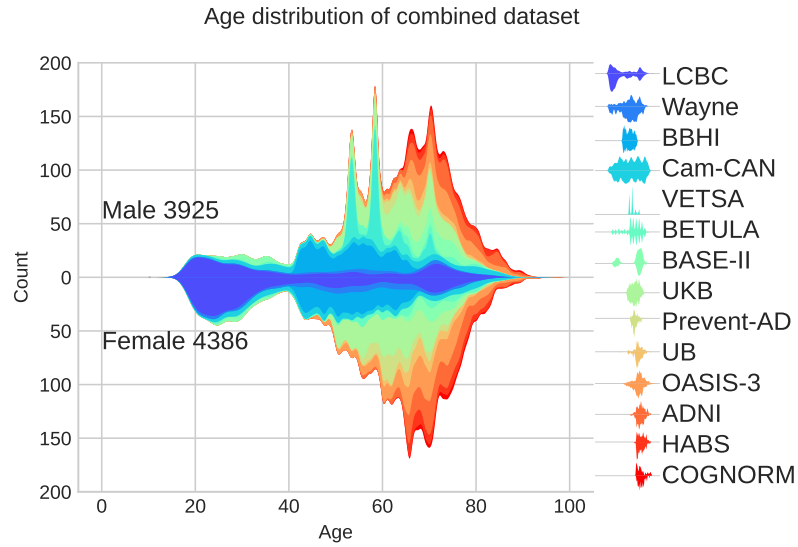


**Figure 6.** Left: Age distribution of the combined sample. The histogram shows the number of male and female participants at each age, with colors denoting different datasets. Right: Age histogram for each dataset with corresponding color.

volume (ICV). There is evidence that ICV —and by extension, brain volume— has increased over the last century (***DeCarli et al., 2024***; ***Kim et al., 2018***). Adjusting for ICV may also correct for other factors such as environmental factors during development and genetics that might bias some of the datasets. To account for these cohort effects, we model the initial brain structure volume at age 18 to be proportional to the ICV. Finally, recognizing that measurements of brain structures are subject to considerable noise and site bias — especially compared to the subtle changes observed over a few years (***Vidal-Piñeiro et al., 2025***) — we explicitly incorporate measurement noise and site bias into our model. We assume that this noise is independent of the other factors influencing brain development, and that each imaging site has a constant bias. With these assumptions, brain development is modeled as a stochastic dynamical system evolving under the influence of both systematic trends and random factors (***Murphy, 2023***).

## Formal Model

We model the system dynamics using the latent state $\boldsymbol{z}(t)$ defined as:

$$\boldsymbol{z}(t) = \begin{bmatrix} s(t) \\ v(t) \end{bmatrix}, \tag{1}$$

with $s(t)$ representing the true volume of the brain structure when removing measurement noise and site bias, and $v(t)$ is the first derivative with respect to time of the volume, which we refer to as change rate. The time variable $t$ denotes the age of the individual, with initial age of $t_0$ being set somewhat arbitrary to the end of development at age 18. Based on the assumption in the previous section the stochastic time continuous dynamical model is given by

$$\begin{aligned} \dot{s}(t) &= v(t), \\ \ddot{s}(t) = \dot{v}(t) &= b(t) + \epsilon_q(t), \end{aligned} \tag{2a}$$

where $(\cdot)$ and $(\cdot\cdot)$ denote the first and second time derivative operation. Here $b(t)$ is an age dependent bias, and $\epsilon_q$ is Gaussian white noise with an age dependent variance $\sigma_q^2(t)$.

The observed volume measurement $\hat{s}(t)$ is modeled as,

$$\hat{s}(t) = s(t) + \beta(\text{site}) + \epsilon_R, \tag{2b}$$

where $\beta(\text{site})$ is a site dependent-bias term. This accounts for different imaging sites have different scanners and scanning protocols that may cause a bias in the volume measurement (***Han et al., 2006***). $\beta$ is constrained such that $\sum_{j \in \text{sites}} \beta_j := 0$, ensuring that $\hat{s}(t)$ is an unbiased estimator of $s(t)$. At time $t_0$ the population latent volume and change rate is modeled as two independent Gaussian distributions,

$$\begin{aligned} s(t_0) &\sim \mathcal{N}(\mu_{s0}(\text{sex}, \text{ICV}), \sigma_{s0}) \\ v(t_0) &\sim \mathcal{N}(\mu_{v0}(\text{sex}, \text{ICV}), \sigma_{v0}) \end{aligned} \tag{2c}$$

where the initial means $\mu_{s0}$ and $\mu_{v0}$ is assumed to be linearly dependent on both the sex and the ICV of the individuals. The variance of the initial distribution of the latent volume and latent change rate is given by $\sigma_{s0}$ and $\sigma_{v0}$. In summary the following parameters are fitted

- Intercept and sex- and ICV-coefficient for mean initial latent volume $\mu_{s0} = \beta_{s0} + \beta_{s0,sex}\text{sex} + \beta_{s0,ICV}\text{ICV}$.
- Intercept and sex- and ICV-coefficient for mean initial change rate $\mu_{v0} = \beta_{v0} + \beta_{v0,sex}\text{sex} + \beta_{v0,ICV}\text{ICV}$.
- Variance term $\sigma_{s0}^2$ for initial latent volume.
- Variance term $\sigma_{v0}^2$ for initial change rate.
- Age dependent bias $b(t)$ for the acceleration parametrized as a cubic spline with 9 check-points.
- Age dependent variance $\sigma_q(t)$ for the acceleration parametrized as a cubic spline with 9 check-points.
- A bias for each site $\beta(\text{site})$.
- Variance term $\sigma_R^2$ for the measurement noise.

This gives a total $12$ parameters when counting the weights of the splines and each site bias as one parameter. When counting all the weights of the splines and the bias for each site there is a total of $66$ fitted parameters.

## Properties of the Stochastic Linear Dynamical System

The model can be expressed compactly in matrix form as:

$$\dot{\boldsymbol{z}}(t) = \boldsymbol{F}\boldsymbol{z}(t) + \boldsymbol{B}(t) + \epsilon_{\boldsymbol{Q}}(t), \qquad \epsilon_{\boldsymbol{Q}}(t) \sim \mathcal{N}(\boldsymbol{0}, \boldsymbol{Q}(t)) \tag{3a}$$

$$\boldsymbol{y}(t) = \boldsymbol{H}\boldsymbol{z}(t) + \boldsymbol{D} + \epsilon_{\boldsymbol{R}}(t), \qquad \epsilon_{\boldsymbol{R}}(t) \sim \mathcal{N}(\boldsymbol{0}, \boldsymbol{R}) \tag{3b}$$

$$\dot{\boldsymbol{z}}(t) = \begin{bmatrix} 0 & 1 \\ 0 & 0 \end{bmatrix} \boldsymbol{z}(t) + \begin{bmatrix} 0 \\ b(t) \end{bmatrix} + \epsilon_{\boldsymbol{Q}}(t), \qquad \epsilon_{\boldsymbol{Q}}(t) \sim \mathcal{N}\left(\boldsymbol{0}, \begin{bmatrix} 0 & 0 \\ 0 & \sigma_q^2(t) \end{bmatrix}\right), \tag{4a}$$

$$\hat{s}(t) = \boldsymbol{y}(t) = \begin{bmatrix} 1 & 0 \end{bmatrix} \boldsymbol{z}(t) + \begin{bmatrix} \beta(\text{site}) \end{bmatrix} + \epsilon_{\boldsymbol{R}}(t), \qquad \epsilon_{\boldsymbol{R}}(t) \sim \mathcal{N}\left(0, \begin{bmatrix} \sigma_R^2 \end{bmatrix}\right), \tag{4b}$$

where $\boldsymbol{y}(t)$ is the measurement vector which in our case is just the measured volume $\hat{s}(t)$. A state-space diagram of the model is shown in Fig. 7.

The continuous model can be time discretized analytically with a sampling period of $\Delta$ (***Driver and Voelkle, 2018***). We assume a zero-order-hold for the time dependent parameters $b(t)$ and $\sigma_q(t)$ within each period $\Delta$ (***Simon, 2006***), meaning these parameters remain constant within this period. Discrete variables are denoted with a star ($*$), and time steps are indexed by $k$, such that $\boldsymbol{F}^*$ represent the time discrete version of $\boldsymbol{F}$ and $b_k := b(t_k)$. The time discrete model is given by

$$\boldsymbol{z}_{k+1} = \boldsymbol{F}^*\boldsymbol{z}_k + \boldsymbol{B}_k^* + \boldsymbol{\epsilon}_{Qk}^*, \qquad \epsilon_{\boldsymbol{Q}^*k} \sim \mathcal{N}\left(\boldsymbol{0}, \boldsymbol{Q}_k^*\right) \tag{5a}$$

$$\boldsymbol{y}_k = \boldsymbol{H}\boldsymbol{z}_k + \boldsymbol{D} + \epsilon_{\boldsymbol{R}k} \qquad \epsilon_{\boldsymbol{R}k} \sim \mathcal{N}(\boldsymbol{0}, \boldsymbol{R}) \tag{5b}$$

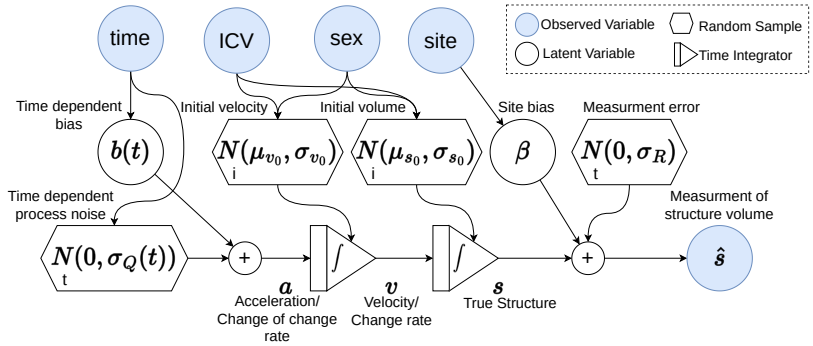


**Figure 7.** State-space diagram showing the dynamical model of the brain structure volume. The $i$ in the hexagon indicates that the variable is iid for each individual, while a $t$ indicates iid for each time step.

$$\boldsymbol{z}_{k+1} = \begin{bmatrix} 1 & \Delta \\ 0 & 1 \end{bmatrix} \boldsymbol{z}_k + \begin{bmatrix} \frac{\Delta^2}{2} b_k \\ \Delta b_k \end{bmatrix} + \epsilon_{\boldsymbol{Q}^* k}, \qquad \epsilon_{\boldsymbol{Q}^* k} \sim \mathcal{N}\left(\boldsymbol{0}, \begin{bmatrix} \frac{\Delta^3}{3}\sigma_{qk} & \frac{\Delta^2}{2}\sigma_{qk} \\ \frac{\Delta^2}{2}\sigma_{qk} & \Delta\sigma_{qk} \end{bmatrix}\right) \tag{6a}$$

$$\boldsymbol{y}_k = \begin{bmatrix} 1 & 0 \end{bmatrix} \boldsymbol{z}_k + \begin{bmatrix} \beta(\text{site}) \end{bmatrix} + \epsilon_{\boldsymbol{R}k}, \qquad \epsilon_{\boldsymbol{R}k} \sim \mathcal{N}\left(0, \begin{bmatrix} \sigma_R^2 \end{bmatrix}\right) \tag{6b}$$

The initial conditions remain as specified in Eq. 2c.

Assume that at time step $k$ the latent state is estimated as $\boldsymbol{z}_k \sim \mathcal{N}(\boldsymbol{\mu}_k, \boldsymbol{\Sigma}_k)$. $\boldsymbol{\mu}_k$ represents the state mean (which can be both the population norm or the mean of an individual's posterior distribution after measurements) and and $\boldsymbol{\Sigma}_k$ denotes the associated uncertainty. The distribution for the subsequent time step is given by

$$\boldsymbol{\mu}_{k+1} = \boldsymbol{F}^* \boldsymbol{\mu}_k + \boldsymbol{B}_k^* \tag{7}$$

$$\boldsymbol{\Sigma}_{k+1} = \boldsymbol{F}^* \boldsymbol{\Sigma}_k \boldsymbol{F}^{*T} + \boldsymbol{Q}_k^* \tag{8}$$

which for $n$ time steps becomes:

$$\boldsymbol{\mu}_{k+n} = \boldsymbol{F}^{*(n)} \boldsymbol{\mu}_k + \sum_{i=0}^{n-1} \boldsymbol{F}^{*(n-1-i)} \boldsymbol{B}_{k+i}^* \tag{9}$$

$$\boldsymbol{\Sigma}_{k+n} = \boldsymbol{F}^{*(n)} \boldsymbol{\Sigma}_k \boldsymbol{F}^{*(n)T} + \sum_{i=0}^{n-1} \boldsymbol{F}^{*(n-1-i)} \boldsymbol{Q}_{k+i}^* \boldsymbol{F}^{*(n-1-i)T} \tag{10}$$

This model puts an important constraint on the system. Since we assuming no correlation between $s(t)$ and $v(t)$ at $t_0$, and no feedback, the variance of $s(t)$ and $v(t)$ will always increase with age. This can easily be verified by writing out the update function of $\boldsymbol{\Sigma}_k$ in Eq. 8 for $\boldsymbol{\Sigma}_k$ with positive off-diagonal terms.

## Correlation Characteristics of the Stochastic Dynamical System

Our goal is to quantify the explained variance of brain structure volume in adulthood given the initial volume at young adulthood $t_0$. To do so we use the auto-correlation (AC) which is the normalized auto-covariance.

The auto-covariance $\boldsymbol{K}$ with lag n is defined as

$$\boldsymbol{K}(\boldsymbol{x}_k, \boldsymbol{x}_{k+n}) = E\left[\left(\boldsymbol{x}_k - E\left[\boldsymbol{x}_k\right]\right)\left(\boldsymbol{x}_{k+n} - E\left[\boldsymbol{x}_{k+n}\right]\right)\right]. \tag{11}$$

We will only consider the case there $n \geq 0$, since the auto-covariance is symmetric for negative $n$ and this simplifies the equations a little. Let $\boldsymbol{d}(\boldsymbol{\Sigma})$ be the vector of the diagonal of a matrix $\boldsymbol{\Sigma}$. We define the standard deviation vector as $\boldsymbol{\sigma} = \sqrt{\boldsymbol{d}(\boldsymbol{\Sigma})}$ and the outer product of this vector as $\overline{\boldsymbol{\Sigma}} = \boldsymbol{\sigma}\boldsymbol{\sigma}^T$. The auto-correlation $\boldsymbol{\rho}_{\text{AC}}$ is given by

$$\boldsymbol{\rho}_{\text{AC}}(\boldsymbol{x}_k, \boldsymbol{x}_{k+n}) = \frac{\boldsymbol{K}(\boldsymbol{x}_k, \boldsymbol{x}_{k+n})}{\sqrt{\overline{\boldsymbol{K}}(\boldsymbol{x}_k, \boldsymbol{x}_k)\overline{\boldsymbol{K}}(\boldsymbol{x}_{k+n}, \boldsymbol{x}_{k+n})}} \tag{12}$$

where the division is performed element-wise. Note that the auto-correlation $\boldsymbol{\rho}_{\mathrm{AC}}$ reduces to the correlation $\boldsymbol{\rho}$ when $n = 0$.

For a linear system such as Eq. 5, the auto-covariance has a closed-form solution given by propagating the initial covariance through the system transfer matrix $\boldsymbol{F}$ $n$ times,

$$\boldsymbol{K}(\boldsymbol{z}_k, \boldsymbol{z}_{k+n}) = \boldsymbol{F}^{*(n)}\boldsymbol{\Sigma}_k \tag{13}$$

$$\boldsymbol{K}(\hat{s}_k, \hat{s}_{k+n}) = \begin{cases} \boldsymbol{H}\boldsymbol{F}^{*(n)}\boldsymbol{\Sigma}_k\boldsymbol{H}^T, & n \neq 0 \\ \boldsymbol{H}\boldsymbol{\Sigma}_k\boldsymbol{H}^T + \boldsymbol{R}, & n = 0 \end{cases} \tag{14}$$

Consequently, $\boldsymbol{\rho}_{\mathrm{AC}}$ for the latent variables can be written compactly as

$$\boldsymbol{\rho}_{\mathrm{AC}}(\boldsymbol{z}_k, \boldsymbol{z}_{k+n}) = \frac{\boldsymbol{F}^{*(n)}\boldsymbol{\Sigma}_k}{\sqrt{\overline{\boldsymbol{\Sigma}}_{k+n}\overline{\boldsymbol{\Sigma}}_k}}. \tag{15}$$

For the observed structures, the measurement noise must be added to the total variance. Thus, $\boldsymbol{\rho}_{\mathrm{AC}}$ for the measurments with $n > 0$ becomes

$$\boldsymbol{\rho}_{\mathrm{AC}}(\hat{s}_k, \hat{s}_{k+n}) = \frac{\boldsymbol{H}\boldsymbol{F}^{*(n)}\boldsymbol{\Sigma}_k\boldsymbol{H}^T}{\sqrt{\left(\boldsymbol{H}\overline{\boldsymbol{\Sigma}}_k\boldsymbol{H}^T + \boldsymbol{R}\right)\left(\boldsymbol{H}\overline{\boldsymbol{\Sigma}}_{k+n}\boldsymbol{H}^T + \boldsymbol{R}\right)}}. \tag{16}$$

We assign names to the elements of Eq. 15 according to their interpretation as correlation coefficients:

$$\boldsymbol{\rho}_{\mathrm{AC}}(\boldsymbol{z}_k, \boldsymbol{z}_{k+n}) = \begin{bmatrix} \rho_{s_k s_{k+n}} & \rho_{v_k s_{k+n}} \\ \rho_{s_k v_{k+n}} & \rho_{v_k v_{k+n}} \end{bmatrix} \tag{17}$$

An intuitive explanation of these coefficients, assuming comparison between time points $k$ and $k + n$, is as follows:

- $\rho_{s_k s_{k+n}}$ is the correlation coefficient of the structure volume at time step $k$ and at the later time step $k + n$.
- $\rho_{v_k s_{k+n}}$ is the correlation coefficient of the change rate at time step $k$ and the volume at the later time step $k + n$.
- $\rho_{s_k v_{k+n}}$ is the correlation coefficient of the volume at time step $k$ and the change rate at the later time step $k + n$.
- $\rho_{v_k v_{k+n}}$ is the correlation coefficient of the change rate at time step $k$ and at the later time step $k + n$.

Often researchers take the time normalized difference between two measurements as a measurement of change rate. We denote this $\hat{v}_{k+n}(n)$ where $n$ denotes the number of time steps between measurements. Here we assume no bias from site.

$$\hat{v}_{k+n}(n) = \frac{1}{n\Delta}\left(\hat{s}_{k+n} - \hat{s}_k\right) \tag{18}$$

The question is whether this is a good measurement of the true change rate at the last time step $k + n$ of the two measurements. We quantify this by calculating the correlation $\rho$ between $\hat{v}_{k+n}(n)$ and $v_{k+n}$ which is given by

$$\rho(\hat{v}_{k+n}, v_{k+n}) = \frac{\boldsymbol{K}(\hat{v}_{k+n}, v_{k+n})}{\sqrt{\boldsymbol{K}(\hat{v}_{k+n}, \hat{v}_{k+n})\boldsymbol{K}(v_{k+n}, v_{k+n})}} \tag{19}$$

A little of mathematical manipulations results in the following expression the the normalized correlation:

$$\rho(\hat{v}_{k+n}, v_{k+n}) = \frac{\boldsymbol{K}(s_{k+n}, v_{k+n}) - \boldsymbol{K}(s_k, v_{k+n})}{\sqrt{(\boldsymbol{K}(\hat{s}_{k+n}, \hat{s}_{k+n}) + \boldsymbol{K}(\hat{s}_k, \hat{s}_k) - 2\boldsymbol{K}(\hat{s}_{k+n}, \hat{s}_k))\boldsymbol{K}(v_{k+n}, v_{k+n})}} \tag{20}$$

which are all quantities that can be calculated from Eq. 13 and Eq. 14.

Another common approach to estimate the change rate, is to do many samples within a period, and use the slope of a linear model as the estimate. Let $\hat{\boldsymbol{s}}_{k:k+n} = \left[\hat{s}_k, \hat{s}_{k+1}, ..., \hat{s}_{k+n}\right]$ be the vector of the equally spaced measurements. It can be shown that the slope $\alpha(\hat{\boldsymbol{s}}_{k:k+n})$ is given by

$$\alpha(\hat{\boldsymbol{s}}_{k:k+n}) = \boldsymbol{\Lambda}\hat{\boldsymbol{s}}_{k:k+n}, \quad \boldsymbol{\Lambda} = \frac{12}{n(n+1)(n+2)}\left[0 - \tfrac{n}{2}, 1 - \tfrac{n}{2}, ..., n - \tfrac{n}{2}\right]. \tag{21}$$

One can thus calculate the correlation as

$$\rho(\alpha(\hat{\boldsymbol{s}}_{k:k+n}), v_{k+n}) = \frac{\boldsymbol{K}(\alpha(\hat{\boldsymbol{s}}_{k:k+n}), v_{k+n})}{\sqrt{\boldsymbol{K}(\alpha(\hat{\boldsymbol{s}}_{k:k+n}), \alpha(\hat{\boldsymbol{s}}_{k:k+n}))\boldsymbol{K}(v_{k+n}, v_{k+n})}} \tag{22}$$

which again with a little mathematical manipulation can be shown to be

$$\rho(\alpha(\hat{\boldsymbol{s}}_{k:k+n}), v_{k+n}) = \frac{\boldsymbol{\Lambda}\boldsymbol{K}(\hat{\boldsymbol{s}}_{k:k+n}, v_{k+n})}{\sqrt{\boldsymbol{\Lambda}\boldsymbol{K}(\hat{\boldsymbol{s}}_{k:k+n}, \hat{\boldsymbol{s}}_{k:k+n})\boldsymbol{\Lambda}^T\boldsymbol{K}(v_{k+n}, v_{k+n})}} \tag{23}$$

Mark that each measurement's contribution to the overall slope is linearly dependent on that measurment's distance in time from the middle time point within the time interval. Therefore, for odd number of observations the middle observations has no contribution to the slope.

## Implementation details

The posterior distribution of the latent variables $p(\boldsymbol{z}_k|y_1...y_K)$ for each individual can be calculated analytically using a Kalman/RTS smoother ***Rauch et al.*** (***1965***); ***Murphy*** (***2023***).

Similarly, the exact likelihood of the longitudinal observations,

$$p(y_0...y_K) = p(y_0)\prod_{k=1}^{K-1} p(y_k|y_0, ..., y_{k-1}) \tag{24}$$

can be evaluated by marginalizing out $\boldsymbol{z}$ using a Kalman filter (***Kalman, 1960***). The model therefore naturally handles both one and multiple observations by calculating the joint probability of all the observations.

In our model we parameterize $q(t_k)$ and $b(t_k)$ as cubic splines with 9 control points, one for every 10 year in the interval 18 to 100. We also tested using 5 and 18 control-points for the splines, without this resulting in any major changes to the results. The volume data was discretized to a sampling interval $\Delta$ of 1.0 year. Here we also tested for intervals of 0.5 years and 2 years, which gave the same results. The priors of the variance terms is parameterized as a squared softplus (***Dugas et al., 2000***) transformed Gaussian distribution.

We use Markov Chain Monte Carlo (MCMC) with a No-U-Turn (NUTS) sampler (***Hoffman et al., 2014***) in order to get the posterior distribution over the model parameters. The model is implemented using the python package Pyro (***Bingham et al., 2019***). The model was first fitted with MAP estimate with a Limited-memory Broyden-Fletcher-Goldfarb-Shanno (L-BFGS) algorithm (***Wright, 2006***). The MCMC sampler was initialized to the MAP estimates, as recommended by ***Geyer*** (***2011***), and 3000 samples was dawned after a warm-up of 500 samples. The trace plots can be examined in Appendix 2.

To improve statistical power and converge rate of the MCMC sampler we used strong priors on the measurement errors of the structures derived from controlled experiments in ***Vidal-Piñeiro et al.*** (***2025***). That is, we centered the priors of $\sigma_R$ around the estimated standard-error for each structure with a standard deviation of 5.0 % of the absolute value of the estimated standard-error. For the other variables we used weak priors that can be examined in Appendix 1.

The combined dataset has a high density of individuals at the age between 50 and 70. To ensure that the analysis was invariant to the age distribution we fitted the model to the data of only LCBC and Cam-CAN, which has a more even age-distribution. This resulted in the same general results as using the full dataset, but with much larger uncertainty in the estimates. These results can be seen in Appendix 4.

## Acknowledgments

This work was supported by South-Eastern Norway Regional Health Authority (to *EG* [HSØ-2021079]), the Department of Psychology, University of Oslo (to *KW*, *AF*), the Norwegian Research Council (to *KW*, *AM*, *DP* [ES694407]) and the project has received funding from the European Research Council's Starting Grant scheme (to *AF*[283634, 725025] and *KW* [313440]).

The different sub-studies are supported by different sources. LCBC: the Norwegian Research Council (to *AF*, *KW*), and the National Association for Public Health's dementia research program (*AF*). Umeå (BETULA): a scholar grant from the Knut and Alice Wallenberg (KAW) foundation to *LN*. UB (Barcelona): *DB-F* was funded by an ICREA Academia Award. *DB-F* acknowledge the CERCA Programme/Generalitat de Catalunya and is supported by María de Maeztu Unit of Excellence (Institute of Neurosciences, University of Barcelona) MDM-2017-0729, Ministry of Science, Innovation and Universities. *LW* and data collection in COGNORM is funded by the South-Eastern Norway Regional Health Authorities [#2017095] The Norwegian Health Association [#19536] and by Wellcome Leap's Dynamic Resilience Program (jointly funded by Temasek Trust) [#104617]. The funding sources had no role in the study design.

Parts of the data collection and sharing for this project was funded by the Alzheimer's Disease Neuroimaging Initiative (ADNI) (National Institutes of Health Grant U01 AG024904) and DOD ADNI (Department of Defense award number W81XWH-12-2-0012). ADNI is funded by the National Institute on Aging, the National Institute of Biomedical Imaging and Bioengineering, and through generous contributions from the following: AbbVie, Alzheimer's Association; Alzheimer's Drug Discovery Foundation; Araclon Biotech; BioClinica, Inc.;Biogen; Bristol-Myers Squibb Company; CereSpir, Inc.; Cogstate; Eisai Inc.; Elan Pharmaceuticals, Inc.; Eli Lilly and Company; EuroImmun; F. Hoffmann-La Roche Ltd and its affiliated company Genentech, Inc.; Fujirebio; GE Healthcare; IXICO Ltd.; Janssen Alzheimer Immunotherapy Research & Development, LLC.; Johnson & Johnson Pharmaceutical Research & Development LLC.; Lumosity; Lundbeck; Merck & Co., Inc.; Meso Scale Diagnostics, LLC.; NeuroRx Research; Neurotrack Technologies; Novartis Pharmaceuticals Corporation; Pfizer Inc.; Piramal Imaging; Servier; Takeda Pharmaceutical Company; and Transition Therapeutics. The Canadian Institutes of Health Research is providing funds to support ADNI clinical sites in Canada. Private sector contributions are facilitated by the Foundation for the National Institutes of Health (www.fnih.org). The grantee organization is the Northern California Institute for Research and Education, and the study is coordinated by the Alzheimer's Therapeutic Research Institute at the University of Southern California. ADNI data are disseminated by the Laboratory for Neuro Imaging at the University of Southern California.

Data used in the preparation of this article were also obtained in part from the Harvard Aging Brain Study (HABS - P01AG036694; https://habs.mgh.harvard.edu). The HABS study was launched in 2010, funded by the National Institute on Aging. and is led by principal investigators Reisa A. Sperling MD and Keith A. Johnson MD at Massachusetts General Hospital/Harvard Medical School in Boston, MA.

OASIS data were provided by OASIS 3: Longitudinal Multimodal Neuroimaging: Principal Investigators: T. Benzinger, D. Marcus, J. Morris; NIH P30 AG066444, P50 AG00561, P30 NS09857781, P01 AG026276, P01 AG003991, R01 AG043434, UL1 TR000448, R01 EB009352. AV-45 doses were provided by Avid Radiopharmaceuticals, a wholly owned subsidiary of Eli Lilly and OASIS-I (test-retest reliability dataset): Cross-Sectional: Principal Investigators: D. Marcus, R, Buckner, J, Csernansky J. Morris; P50 AG05681, P01 AG03991, P01 AG026276, R01 AG021910, P20 MH071616, U24 RR021382. PREVENT-AD was funded by the Canadian Institutes of Health Research, McGill University, the Fonds de Recherche du Québec – Santé, Alzheimer's Association, Brain Canada, the Government of Canada, the Canada Fund for Innovation, the Douglas Hospital Research Centre and Foundation, the Levesque Foundation, an unrestricted research grant from Pfizer Canada. Private sector contributions are facilitated by the Development Office of the McGill University Faculty of Medicine and by the Douglas Hospital Research Centre Foundation (http://www.douglas.qc.ca/).

UK Biobank is generously supported by its founding funders the Wellcome Trust and UK Medical Research Council, as well as the Department of Health, Scottish Government, the Northwest Regional Development Agency, British Heart Foundation and Cancer Research UK. The organisation has over 150 dedicated members of staff, based in multiple locations across the UK.

Parts of the data are from VETSA, which is funded by the National Institute of Aging grants R01s AG018384, AG018386, AG050595, AG022381, AG076838. The content is the responsibility of the authors and does not necessarily represent official views of the NIA, NIH, or VA. U.S. Department of Veterans Affairs, Department of Defense; National Personnel Records Center, National Archives and Records Administration; Internal Revenue Service; National Opinion Research Center; National Research Council, National Academy of Sciences; and the Institute for Survey Research, Temple University provided invaluable assistance in the conduct of the VET Registry. The Cooperative Studies Program of the U.S. Department of Veterans Affairs provided financial support for development and maintenance of the Vietnam Era Twin Registry. We would also like to acknowledge the continued cooperation and participation of the members of the VET Registry and their families.

## Author Contributions

Conceptualization: AF, DP and EG. Data curation: DP. Formal analysis: EG, DP and ØS. Funding acquisition: AF and AB. Investigation: DB-F, AB, GC, SD, RH, SK, UL, LN, AP-L, CS-P, JS, LW and KW. Methodology: EG, AD, DP, SS, BM and PG. Supervision: BM, AF and AB. Project administration: AF and AB. Resources: AF and AB. Visualization: EG. Writing – original draft: EG, AF and DP. Writing – review and editing: All authors

## References

**Abé C**, Ching CR, Liberg B, Lebedev AV, Agartz I, Akudjedu TN, Alda M, Alnæs D, Alonso-Lana S, Benedetti F, et al. Longitudinal structural brain changes in bipolar disorder: a multicenter neuroimaging study of 1232 individuals by the ENIGMA bipolar disorder working group. Biological psychiatry. 2022; 91(6):582–592.

**Abellaneda-Pérez K**, Vaqué-Alcázar L, Vidal-Piñeiro D, Jannati A, Solana E, Bargalló N, Santarnecchi E, Pascual-Leone A, Bartrés-Faz D. Age-related differences in default-mode network connectivity in response to intermittent theta-burst stimulation and its relationships with maintained cognition and brain integrity in healthy aging. Neuroimage. 2019; 188:794–806.

**Allen JS**, Bruss J, Brown CK, Damasio H. Normal neuroanatomical variation due to age: the major lobes and a parcellation of the temporal region. Neurobiology of aging. 2005; 26(9):1245–1260.

**Ballester PL**, Suh JS, Ho NC, Liang L, Hassel S, Strother SC, Arnott SR, Minuzzi L, Sassi RB, Lam RW, et al. Gray matter volume drives the brain age gap in schizophrenia: a SHAP study. Schizophrenia. 2023; 9(1):3.

**Bashyam VM**, Erus G, Doshi J, Habes M, Nasrallah IM, Truelove-Hill M, Srinivasan D, Mamourian L, Pomponio R, Fan Y, et al. MRI signatures of brain age and disease over the lifespan based on a deep brain network and 14 468 individuals worldwide. Brain. 2020; 143(7):2312–2324.

**Bertram L**, Böckenhoff A, Demuth I, Düzel S, Eckardt R, Li SC, Lindenberger U, Pawelec G, Siedler T, Wagner GG, et al. Cohort profile: the Berlin aging study II (BASE-II). International journal of epidemiology. 2014; 43(3):703–712.

**Bingham E**, Chen JP, Jankowiak M, Obermeyer F, Pradhan N, Karaletsos T, Singh R, Szerlip P, Horsfall P, Goodman ND. Pyro: Deep universal probabilistic programming. Journal of machine learning research. 2019; 20(28):1–6.

**Blake KV**, Ntwatwa Z, Kaufmann T, Stein DJ, Ipser JC, Groenewold NA. Advanced brain ageing in adult psychopathology: A systematic review and meta-analysis of structural MRI studies. Journal of psychiatric research. 2023; 157:180–191.

**Brandmaier AM**, Lindenberger U, McCormick EM. Optimal two-time point longitudinal models for estimating individual-level change: Asymptotic insights and practical implications. Developmental Cognitive Neuroscience. 2024; 70:101450.

**Brandmaier AM**, Von Oertzen T, Ghisletta P, Lindenberger U, Hertzog C. Precision, reliability, and effect size of slope variance in latent growth curve models: Implications for statistical power analysis. Frontiers in Psychology. 2018; 9:294.

**Brandmaier AM**, Wenger E, Bodammer NC, Kühn S, Raz N, Lindenberger U. Assessing reliability in neuroimaging research through intra-class effect decomposition (ICED). Elife. 2018; 7:e35718.

**Bråthen ACS**, Sørensen Ø, De Lange AMG, Mowinckel AM, Fjell AM, Walhovd KB. Cognitive and hippocampal changes weeks and years after memory training. Scientific Reports. 2022; 12(1):7877.

**Burgmans S**, van Boxtel MP, Gronenschild E, Vuurman E, Hofman P, Uylings HB, Jolles J, Raz N. Multiple indicators of age-related differences in cerebral white matter and the modifying effects of hypertension. Neuroimage. 2010; 49(3):2083–2093.

**Cattaneo G**, Bartrés-Faz D, Morris TP, Sánchez JS, Macià D, Tarrero C, Tormos JM, Pascual-Leone A. The Barcelona brain health initiative: a cohort study to define and promote determinants of brain health. Frontiers in Aging Neuroscience. 2018; 10:321.

**Cole JH**, Ritchie SJ, Bastin ME, Hernández V, Muñoz Maniega S, Royle N, Corley J, Pattie A, Harris SE, Zhang Q, et al. Brain age predicts mortality. Molecular psychiatry. 2018; 23(5):1385–1392.

**Constantinides C**, Han LK, Alloza C, Antonucci LA, Arango C, Ayesa-Arriola R, Banaj N, Bertolino A, Borgwardt S, Bruggemann J, et al. Brain ageing in schizophrenia: evidence from 26 international cohorts via the ENIGMA Schizophrenia consortium. Molecular psychiatry. 2023; 28(3):1201–1209.

**Dagley A**, LaPoint M, Huijbers W, Hedden T, McLaren DG, Chatwal JP, Papp KV, Amariglio RE, Blacker D, Rentz DM, et al. Harvard aging brain study: dataset and accessibility. Neuroimage. 2017; 144:255–258.

**DeCarli C**, Maillard P, Pase MP, Beiser AS, Kojis D, Satizabal CL, Himali JJ, Aparicio HJ, Fletcher E, Seshadri S. Trends in intracranial and cerebral volumes of Framingham heart study participants born 1930 to 1970. JAMA neurology. 2024; 81(5):471–480.

**Dörfel RP**, Ozenne B, Ganz M, Svensson J, Plavén-Sigray P. Prediction of brain age using structural magnetic resonance imaging: A comparison of clinical validity of publicly available software packages. medRxiv. 2025; p. 2025–03.

**Driscoll I**, Davatzikos C, An Y, Wu X, Shen D, Kraut M, Resnick S. Longitudinal pattern of regional brain volume change differentiates normal aging from MCI. Neurology. 2009; 72(22):1906–1913.

**Driver CC**, Voelkle MC. Hierarchical Bayesian continuous time dynamic modeling. Psychological methods. 2018; 23(4):774.

**Dugas C**, Bengio Y, Bélisle F, Nadeau C, Garcia R. Incorporating second-order functional knowledge for better option pricing. Advances in neural information processing systems. 2000; 13.

**Einstein A**. On the theory of the Brownian movement. Ann Phys. 1906; 19(4):371–381.

**Elliott ML**, Du JL, Nielsen JA, Hanford LC, Kivisakk P, Arnold SE, Dickerson BC, Mair RW, Eldaief MC, Buckner RL. Precision Estimates of Longitudinal Brain Aging Capture Unexpected Individual Differences in One Year. medRxiv. 2025; p. 2025–02.

**Elliott ML**, Nielsen JA, Hanford LC, Hamadeh A, Hilbert T, Kober T, Dickerson BC, Hyman BT, Mair RW, Eldaief MC, et al. Precision brain morphometry using cluster scanning. Imaging Neuroscience. 2024; 2:1–15.

**Engvig A**, Fjell AM, Westlye LT, Moberget T, Sundseth Ø, Larsen VA, Walhovd KB. Effects of memory training on cortical thickness in the elderly. Neuroimage. 2010; 52(4):1667–1676.

**Fjell AM**, Walhovd KB, Fennema-Notestine C, McEvoy LK, Hagler DJ, Holland D, Brewer JB, Dale AM. One-year brain atrophy evident in healthy aging. Journal of Neuroscience. 2009; 29(48):15223–15231.

**Fjell AM**, Westlye LT, Grydeland H, Amlien I, Espeseth T, Reinvang I, Raz N, Holland D, Dale AM, Walhovd KB, et al. Critical ages in the life course of the adult brain: nonlinear subcortical aging. Neurobiology of aging. 2013; 34(10):2239–2247.

**Föllmer H**, Schied A. Stochastic finance: an introduction in discrete time. Walter de Gruyter; 2011.

**Franke K**, Gaser C. Ten years of BrainAGE as a neuroimaging biomarker of brain aging: what insights have we gained? Frontiers in neurology. 2019; 10:789.

**Friston K**. The free-energy principle: a unified brain theory? Nature reviews neuroscience. 2010; 11(2):127–138.

**Fürtjes AE**, Foote IF, Xia C, Davies G, Moodie J, Taylor A, Liewald DC, Redmond P, Corley J, McIntosh AM, et al. Lifetime brain atrophy estimated from a single MRI: measurement characteristics and genome-wide correlates. bioRxiv. 2024; .

**Gardiner CW**, et al. Handbook of stochastic methods, vol. 3. springer Berlin; 1985.

**Geyer CJ**. Introduction to markov chain monte carlo. Handbook of markov chain monte carlo. 2011; 20116022(45):22.

**Ghisletta P**, Mason F, von Oertzen T, Hertzog C, Nilsson LG, Lindenberger U. On the use of growth models to study normal cognitive aging. International Journal of Behavioral Development. 2020; 44(1):88–96.

**Habes M**, Janowitz D, Erus G, Toledo J, Resnick S, Doshi J, Van der Auwera S, Wittfeld K, Hegenscheid K, Hosten N, et al. Advanced brain aging: relationship with epidemiologic and genetic risk factors, and overlap with Alzheimer disease atrophy patterns. Translational psychiatry. 2016; 6(4):e775–e775.

**Han LK**, Dinga R, Hahn T, Ching CR, Eyler LT, Aftanas L, Aghajani M, Aleman A, Baune BT, Berger K, et al. Brain aging in major depressive disorder: results from the ENIGMA major depressive disorder working group. Molecular psychiatry. 2021; 26(9):5124–5139.

**Han X**, Jovicich J, Salat D, van der Kouwe A, Quinn B, Czanner S, Busa E, Pacheco J, Albert M, Killiany R, et al. Reliability of MRI-derived measurements of human cerebral cortical thickness: the effects of field strength, scanner upgrade and manufacturer. Neuroimage. 2006; 32(1):180–194.

**Hertzog C**, von Oertzen T, Ghisletta P, Lindenberger U. Evaluating the power of latent growth curve models to detect individual differences in change. Structural Equation Modeling: A Multidisciplinary Journal. 2008; 15(4):541–563.

**Hoffman MD**, Gelman A, et al. The No-U-Turn sampler: adaptively setting path lengths in Hamiltonian Monte Carlo. J Mach Learn Res. 2014; 15(1):1593–1623.

**Hoogman M**, Bralten J, Hibar DP, Mennes M, Zwiers MP, Schweren LS, van Hulzen KJ, Medland SE, Shumskaya E, Jahanshad N, et al. Subcortical brain volume differences in participants with attention deficit hyperactivity disorder in children and adults: a cross-sectional mega-analysis. The Lancet Psychiatry. 2017; 4(4):310–319.

**Idland AV**, Sala-Llonch R, Borza T, Watne LO, Wyller TB, Brækhus A, Zetterberg H, Blennow K, Walhovd KB, Fjell AM. CSF neurofilament light levels predict hippocampal atrophy in cognitively healthy older adults. Neurobiology of aging. 2017; 49:138–144.

**Kalman RE**. A New Approach to Linear Filtering and Prediction Problems. Journal of Basic Engineering. 1960 03; 82(1):35–45. https://doi.org/10.1115/1.3662552, doi: 10.1115/1.3662552.

**Kennedy KM**, Raz N. Aging white matter and cognition: differential effects of regional variations in diffusion properties on memory, executive functions, and speed. Neuropsychologia. 2009; 47(3):916–927.

**Kim YS**, Park IS, Kim HJ, Kim D, Lee NJ, Rhyu IJ. Changes in intracranial volume and cranial shape in modern Koreans over four decades. American journal of physical anthropology. 2018; 166(3):753–759.

**Korbmacher M**, Vidal-Pineiro D, Wang MY, van der Meer D, Wolfers T, Nakua H, Eikefjord E, Andreassen OA, Westlye LT, Maximov II. Cross-sectional brain age assessments are limited in predicting future brain change. bioRxiv. 2024; p. 2024–09.

**Kremen WS**, Franz CE, Lyons MJ. Current status of the Vietnam era twin study of aging (VETSA). Twin Research and Human Genetics. 2019; 22(6):783–787.

**LaMontagne PJ**, Benzinger TL, Morris JC, Keefe S, Hornbeck R, Xiong C, Grant E, Hassenstab J, Moulder K, Vlassenko AG, et al. OASIS-3: longitudinal neuroimaging, clinical, and cognitive dataset for normal aging and Alzheimer disease. medrxiv. 2019; p. 2019–12.

**Lee U**. Do stock prices follow random walk?:: Some international evidence. International Review of Economics & Finance. 1992; 1(4):315–327.

**Lindenberger U**, Von Oertzen T, Ghisletta P, Hertzog C. Cross-sectional age variance extraction: what's change got to do with it? Psychology and aging. 2011; 26(1):34.

**Livingston G**, Huntley J, Liu KY, Costafreda SG, Selbæk G, Alladi S, Ames D, Banerjee S, Burns A, Brayne C, et al. Dementia prevention, intervention, and care: 2024 report of the Lancet standing Commission. The Lancet. 2024; 404(10452):572–628.

**McElreath R**. Statistical rethinking: A Bayesian course with examples in R and Stan. Chapman and Hall/CRC; 2018.

**Miller KL**, Alfaro-Almagro F, Bangerter NK, Thomas DL, Yacoub E, Xu J, Bartsch AJ, Jbabdi S, Sotiropoulos SN, Andersson JL, et al. Multimodal population brain imaging in the UK Biobank prospective epidemiological study. Nature neuroscience. 2016; 19(11):1523–1536.

**Mueller SG**, Weiner MW, Thal LJ, Petersen RC, Jack C, Jagust W, Trojanowski JQ, Toga AW, Beckett L. The Alzheimer's disease neuroimaging initiative. Neuroimaging Clinics. 2005; 15(4):869–877.

**Murphy KP**. Probabilistic Machine Learning: Advanced Topics. MIT Press; 2023. http://probml.github.io/book2.

**Nilsson LG**, Adolfsson R, Bäckman L, de Frias CM, Molander B, Nyberg L. Betula: A prospective cohort study on memory, health and aging. Aging Neuropsychology and Cognition. 2004; 11(2-3):134–148.

**Nilsson LG**, BÄCkman L, Erngrund K, Nyberg L, Adolfsson R, Bucht G, Karlsson S, Widing M, Winblad B. The Betula prospective cohort study: Memory, health, and aging. Aging, Neuropsychology, and Cognition. 1997; 4(1):1–32.

**Nyberg L**, Magnussen F, Lundquist A, Baaré W, Bartrés-Faz D, Bertram L, Boraxbekk CJ, Brandmaier AM, Drevon CA, Ebmeier K, et al. Educational attainment does not influence brain aging. Proceedings of the National Academy of Sciences. 2021; 118(18):e2101644118.

**Nyberg L**, Salami A, Andersson M, Eriksson J, Kalpouzos G, Kauppi K, Lind J, Pudas S, Persson J, Nilsson LG. Longitudinal evidence for diminished frontal cortex function in aging. Proceedings of the National Academy of Sciences. 2010; 107(52):22682–22686.

**Preacher KJ**. Latent growth curve modeling. No. 157, Sage; 2008.

**Rajaram S**, Valls-Pedret C, Cofán M, Sabaté J, Serra-Mir M, Pérez-Heras AM, Arechiga A, Casaroli-Marano RP, Alforja S, Sala-Vila A, et al. The Walnuts and Healthy Aging Study (WAHA): protocol for a nutritional intervention trial with walnuts on brain aging. Frontiers in aging neuroscience. 2017; 8:333.

**Rauch HE**, Tung F, Striebel CT. Maximum likelihood estimates of linear dynamic systems. AIAA journal. 1965; 3(8):1445–1450.

**Raz N**, Lindenberger U. Only time will tell: Cross-sectional studies offer no solution to the age–brain–cognition triangle: Comment on Salthouse (2011). Psychological Bulletin. 2011; .

**Raz N**, Lindenberger U, Rodrigue KM, Kennedy KM, Head D, Williamson A, Dahle C, Gerstorf D, Acker JD. Regional brain changes in aging healthy adults: general trends, individual differences and modifiers. Cerebral cortex. 2005; 15(11):1676–1689.

**Reuter M**, Schmansky NJ, Rosas HD, Fischl B. Within-subject template estimation for unbiased longitudinal image analysis. Neuroimage. 2012; 61(4):1402–1418.

**Rohrer JM**. Thinking Clearly About Age, Period, and Cohort Effects. PsyArXiv Preprints. 2025; .

**Sele S**, Liem F, Mérillat S, Jäncke L. Age-related decline in the brain: a longitudinal study on inter-individual variability of cortical thickness, area, volume, and cognition. Neuroimage. 2021; 240:118370.

**Shafto MA**, Tyler LK, Dixon M, Taylor JR, Rowe JB, Cusack R, Calder AJ, Marslen-Wilson WD, Duncan J, Dalgleish T, et al. The Cambridge Centre for Ageing and Neuroscience (Cam-CAN) study protocol: a cross-sectional, lifespan, multidisciplinary examination of healthy cognitive ageing. BMC neurology. 2014; 14:1–25.

**Simon D**. Optimal state estimation: Kalman, H infinity, and nonlinear approaches. John Wiley & Sons; 2006.

**Smith SM**, Elliott LT, Alfaro-Almagro F, McCarthy P, Nichols TE, Douaud G, Miller KL. Brain aging comprises many modes of structural and functional change with distinct genetic and biophysical associations. elife. 2020; 9:e52677.

**Smith SM**, Miller KL, Nichols TE. Characterising ongoing brain aging from cross-sectional data. bioRxiv. 2025; p. 2025–01.

**Smith SM**, Vidaurre D, Alfaro-Almagro F, Nichols TE, Miller KL. Estimation of brain age delta from brain imaging. Neuroimage. 2019; 200:528–539.

**Sørensen Ø**, McCormick EM. Modeling Cycles, Trends and Time-Varying Effects in Dynamic Structural Equation Models with Regression Splines. PsyArXiv Preprints. 2025; .

**Tremblay-Mercier J**, Madjar C, Das S, Binette AP, Dyke SO, Étienne P, Lafaille-Magnan ME, Remz J, Bellec P, Collins DL, et al. Open science datasets from PREVENT-AD, a longitudinal cohort of pre-symptomatic Alzheimer's disease. NeuroImage: Clinical. 2021; 31:102733.

**Uribe C**, Segura B, Baggio HC, Abos A, Marti MJ, Valldeoriola F, Compta Y, Bargallo N, Junque C. Patterns of cortical thinning in nondemented Parkinson's disease patients. Movement Disorders. 2016; 31(5):699–708.

**Van Erp TG**, Walton E, Hibar DP, Schmaal L, Jiang W, Glahn DC, Pearlson GD, Yao N, Fukunaga M, Hashimoto R, et al. Cortical brain abnormalities in 4474 individuals with schizophrenia and 5098 control subjects via the enhancing neuro imaging genetics through meta analysis (ENIGMA) consortium. Biological psychiatry. 2018; 84(9):644–654.

**Vidal-Piñeiro D**, Martin-Trias P, Arenaza-Urquijo EM, Sala-Llonch R, Clemente IC, Mena-Sánchez I, Bargalló N, Falcón C, Pascual-Leone Á, Bartrés-Faz D. Task-dependent activity and connectivity predict episodic memory network-based responses to brain stimulation in healthy aging. Brain stimulation. 2014; 7(2):287–296.

**Vidal-Piñeiro D**, Sørensen Ø, Strømstad M, Amlien IK, Anderson M, Baaré WF, Bartrés-Faz D, Brandmaier AM, Bråthen AC, Garrido P, et al. Reliability of structural brain change in cognitively healthy adult samples. Imaging Neuroscience. 2025; .

**Vidal-Pineiro D**, Wang Y, Krogsrud SK, Amlien IK, Baaré WF, Bartres-Faz D, Bertram L, Brandmaier AM, Drevon CA, Düzel S, et al. Individual variations in 'brain age'relate to early-life factors more than to longitudinal brain change. elife. 2021; 10:e69995.

**Vita A**, De Peri L, Deste G, Sacchetti E. Progressive loss of cortical gray matter in schizophrenia: a meta-analysis and meta-regression of longitudinal MRI studies. Translational psychiatry. 2012; 2(11):e190–e190.

**Walhovd KB**, Fjell AM, Brown TT, Kuperman JM, Chung Y, Hagler Jr DJ, Roddey JC, Erhart M, McCabe C, Akshoomoff N, et al. Long-term influence of normal variation in neonatal characteristics on human brain development. Proceedings of the National Academy of Sciences. 2012; 109(49):20089–20094.

**Walhovd KB**, Fjell AM, Reinvang I, Lundervold A, Dale AM, Eilertsen DE, Quinn BT, Salat D, Makris N, Fischl B. Effects of age on volumes of cortex, white matter and subcortical structures. Neurobiology of aging. 2005; 26(9):1261–1270.

**Walhovd KB**, Fjell AM, Westerhausen R, Nyberg L, Ebmeier KP, Lindenberger U, Bartrés-Faz D, Baaré WF, Siebner HR, Henson R, et al. Healthy minds 0–100 years: Optimising the use of European brain imaging cohorts ("Lifebrain"). European Psychiatry. 2018; 50:47–56.

**Walhovd KB**, Krogsrud SK, Amlien IK, Bartsch H, Bjørnerud A, Due-Tønnessen P, Grydeland H, Hagler Jr DJ, Håberg AK, Kremen WS, et al. Neurodevelopmental origins of lifespan changes in brain and cognition. Proceedings of the National Academy of Sciences. 2016; 113(33):9357–9362.

**Walhovd KB**, Lövden M, Fjell AM. Timing of lifespan influences on brain and cognition. Trends in cognitive sciences. 2023; 27(10):901–915.

**Walhovd KB**, Nyberg L, Lindenberger U, Amlien IK, Sørensen Ø, Wang Y, Mowinckel AM, Kievit RA, Ebmeier KP, Bartrés-Faz D, et al. Brain aging differs with cognitive ability regardless of education. Scientific reports. 2022; 12(1):13886.

**Walhovd KB**, Westlye LT, Amlien I, Espeseth T, Reinvang I, Raz N, Agartz I, Salat DH, Greve DN, Fischl B, et al. Consistent neuroanatomical age-related volume differences across multiple samples. Neurobiology of aging. 2011; 32(5):916–932.

**Welch G**, Bishop G, et al., An introduction to the Kalman filter. Chapel Hill, NC, USA; 1995.

**Wenger E**, Kühn S, Verrel J, Mårtensson J, Bodammer NC, Lindenberger U, Lövdén M. Repeated structural imaging reveals nonlinear progression of experience-dependent volume changes in human motor cortex. Cerebral Cortex. 2017; 27(5):2911–2925.

**Wenger E**, Schaefer S, Noack H, Kühn S, Mårtensson J, Heinze HJ, Düzel E, Bäckman L, Lindenberger U, Lövdén M. Cortical thickness changes following spatial navigation training in adulthood and aging. Neuroimage. 2012; 59(4):3389–3397.

**Wright SJ**, Numerical optimization; 2006.

**Zhu JD**, Wu YF, Tsai SJ, Lin CP, Yang AC. Investigating brain aging trajectory deviations in different brain regions of individuals with schizophrenia using multimodal magnetic resonance imaging and brain-age prediction: a multicenter study. Translational Psychiatry. 2023; 13(1):82.

# Appendix 1

## Priors

Before fitting the model each structure is z-scored such that the whole dataset population has a mean of 0 and a std of 1. The priors are set in the z-scored units such that the same priors relative to the scale of each structure is used. The time is normalized to [0, 1] such that a for instance the prior of initial change rate $\beta_{v0} \sim \mathcal{N}(0, 5)$ corresponds to a prior covering the change rates from -10 std to +10 std over the life span, when considering the 95% CI. Notice that the priors on the $b(t)$ corresponds to the common L2 smoothing priors for splines.

| Parameter | Prior Distribution | Comments |
|---|---|---|
| $b(t)$ | $\mathcal{N}(0, 10)$ | |
| $\sigma_q(t)$ | $\mathrm{Softplus}\Big(\mathcal{N}(a, b)\Big)$ | such that $E[\sigma_q] \approx 10$, $Std[\sigma_q] \approx 10$ |
| $\beta_{s0}$ | $\mathcal{N}(0, 5)$ | |
| $\beta_{v0}$ | $\mathcal{N}(0, 5)$ | |
| $\sigma_{s0}$ | $\mathrm{Softplus}\Big(\mathcal{N}(a, b)\Big)$ | such that $E[\sigma_{s0}] \approx 2$, $Std[\sigma_{s0}] \approx 2$ |
| $\sigma_{v0}$ | $\mathrm{Softplus}\Big(\mathcal{N}(a, b)\Big)$ | such that $E[\sigma_{v0}] \approx 2$, $Std[\sigma_{v0}] \approx 2$ |
| $\beta_{s0,\mathrm{sex}}$ | $\mathcal{N}(0, 0.2)$ | |
| $\beta_{s0,\mathrm{lCV}}$ | $\mathcal{N}(0, 1.0)$ | |
| $\beta_{v0,\mathrm{sex}}$ | $\mathcal{N}(0, 0.01)$ | |
| $\beta_{v0,\mathrm{lCV}}$ | $\mathcal{N}(0, 0.01)$ | |
| $\sigma_R$ | $\mathrm{Softplus}\Big(\mathcal{N}(a, b)\Big)$ | such that $E[\sigma_R] \approx \sigma_{q,\mathrm{emp}}$, $Std[\sigma_R] \approx 0.05\,\sigma_{q,\mathrm{emp}}$ |
| $\beta(\mathrm{site})$ | $\mathcal{N}(0, 0.3)$ | with $\sum_{site \in \mathrm{sites}} \beta(site) = 0$ |

# Appendix 2

## Trace Plots

The trace plots of our MCMC runs, to show proper convergence and coverage of the posterior distribution ***Geyer*** (***2011***).

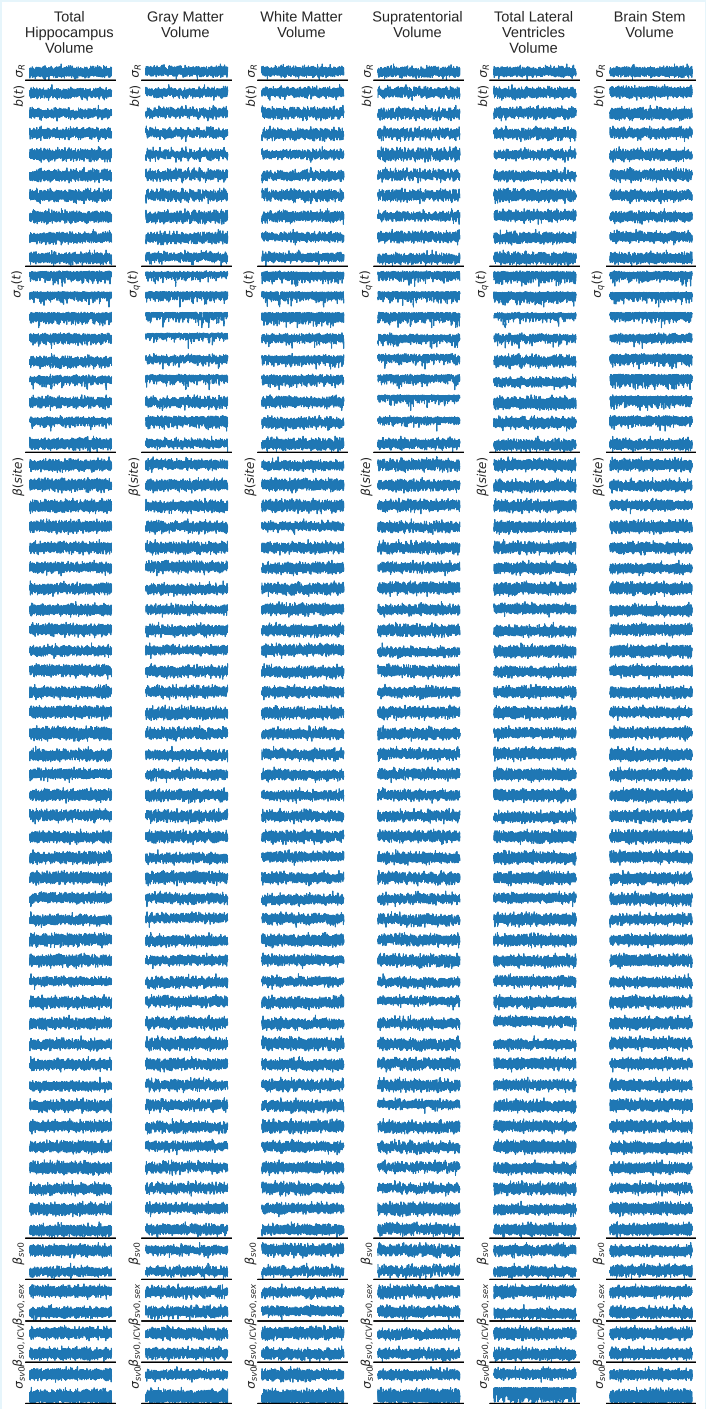


**Appendix 2—figure 1.** Trace plot of the MCMC runs. The parameters of the initial conditions are grouped together such that the first plot shows the latent structure volume parameter and the second the change rate.

# Appendix 3

## Significance Tests

In order to make statements on properties of the shape of the population trajectories we performed statistical test for significance. For all ages we test for significant differences in values for the change rate and acceleration of the model. For each sample of the MCMC trace we compared if more than 97.5% or 99.9% of the samples where either over or under that of another age. Similar tests was performed for $b(t)$ being different from zero. For the structure volume curves, the uncertainty was so low that we have not included them in this plot, but a visual inspection of Fig. 1 can verify this.

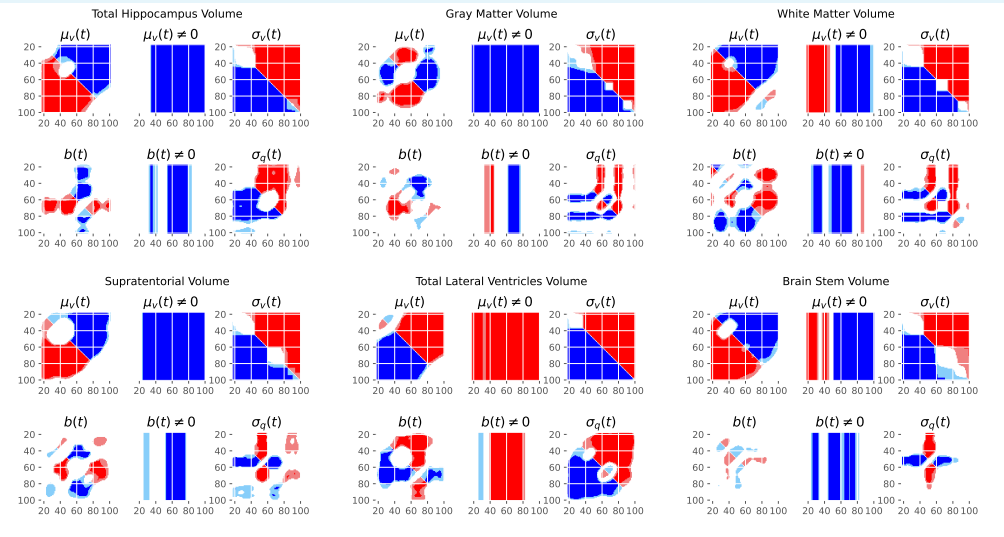


**Appendix 3—figure 1.** Significance plots for the time dependent parameters. The x-axes indicate the age to compare from and the y-axes the age to compare to. Blue indicate significantly smaller, and red significantly larger. Light colors show $0.025 > p > 0.001$ and saturated colors $p < 0.001$ Example on how to read: take $b(t)$ for white matter. We choose to compare the age of 60 to all other ages. We then look at the vertical line up from 60, and we see that at 60 the mean acceleration $b(t)$ is significantly smaller than the acceleration at 80 to 90 and the acceleration at 40. There is no significant differences between the acceleration at 60 and the acceleration at for instance 30.

# Appendix 4

## Verification of Invariance to Dataset Distribution

In Fig. 1 as well as in Fig. 6 one can notice that the age group from 50 to 70 has a higher representation than the younger age group. We also see that the spread of the variance in change rate happens at the beginning of this high density of data. To make sure that this is not an artifact of the age distribution of the sample we performed a second fit to a subsample for the data. The subsample consisted of the LCBC dataset and Cam-CAN dataset, which both have even age distribution. We observe that the confidence intervals for the normative curves are wider than for the full dataset, as expected, however we see no significant differences to the conclusions drawn from the full dataset. We therefore conclude that the the spread of change rate variance at age 50 is not due to an artifact of age distribution.

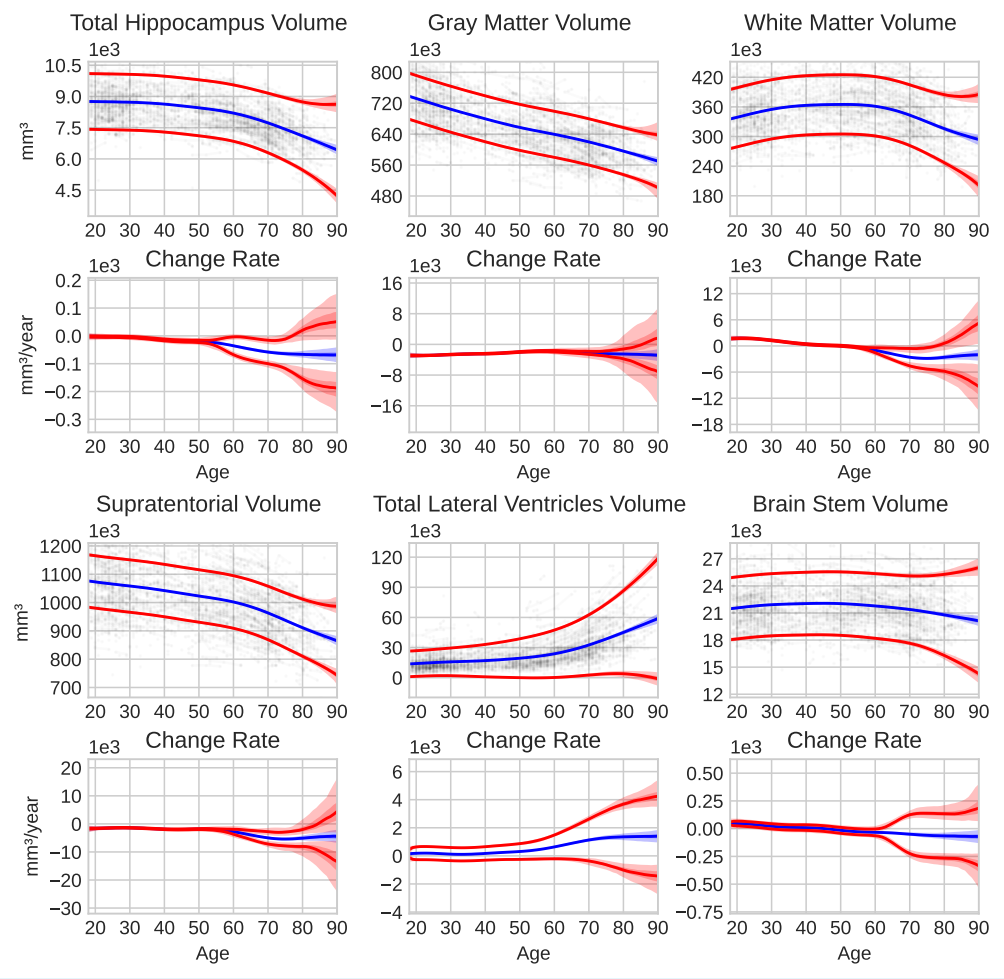


**Appendix 4—figure 1.** Reproduction of the Fig. 1 however here only data from the LCBC dataset and Cam-CAN is used to fit the model such that the the age distribution is more uniform. The CI around the lines are much wider, especially for older ages and the axis are adjusted to include the full CI.

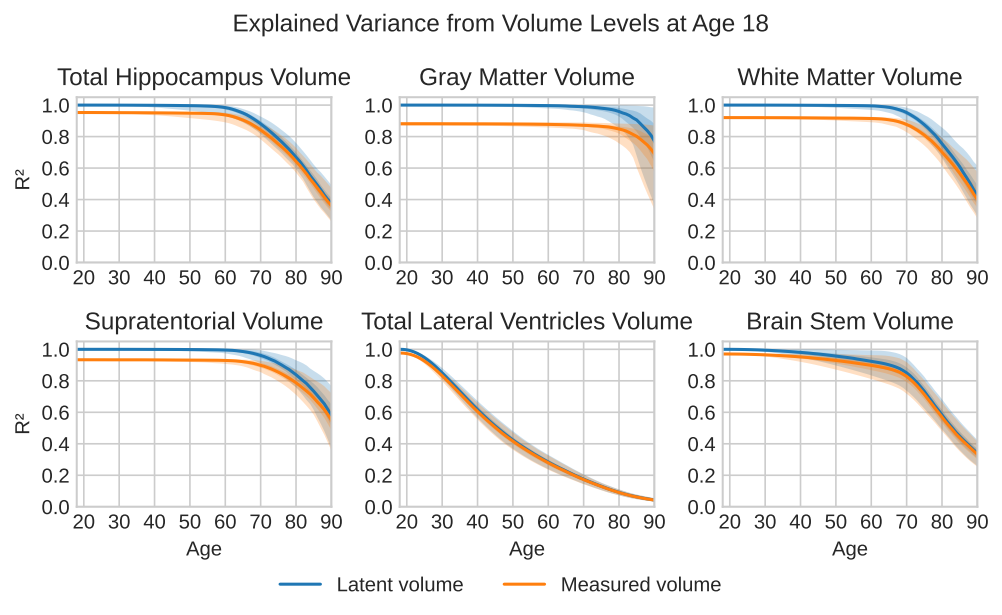


**Appendix 4—figure 2.** Reproduction of the Fig. 2 however here only data from the LCBC dataset and Cam-CAN is used to fit the model.

# Appendix 5

## Standard Deviation of the Brain structure Volumes

We plotted the standard deviation (SD) for age bins of 1 year throughout the adult lifespan. We observe that for all structures, except the ventricles, the SD is stable throughout the lifespan, with possibly a small tendency to shrink after the age of 60 years in the case of the Total Gray Matter Volume and the Supratentorial Volume. If individuals have large variation in trajectories one would expect the SD to increase with time, not remain stable as seen here. As discussed in the discussion, when the model is fitted to the data, this is likely some of the evidence that is taken into account when estimating the model parameters, and hence low variation in change is a likely senario given the model.

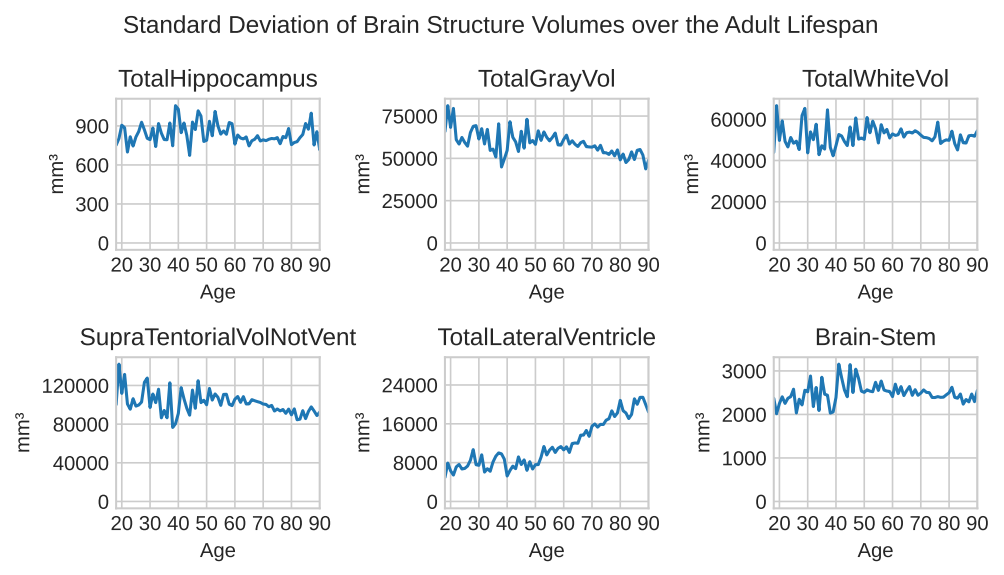


**Appendix 5—figure 1.** Standard deviation of the volume of the brain structures throughout the adult lifespan.